Palaeogeography, Palaeoclimatology, Palaeoecology 427 (2015) 1–19

Contents lists available at ScienceDirect

Palaeogeography, Palaeoclimatology, Palaeoecology

journal homepage: www.elsevier.com/locate/palaeo

Uppermost Devonian (Famennian) to Lower Mississippian events of the western U.S.: Stratigraphy, sedimentology, chemostratigraphy, and detrital zircon geochronology

D. Cole [a,*], P.M. Myrow [a,1], D.A. Fike [b], A. Hakim [a], G.E. Gehrels [c]

[a] Department of Geology, Colorado College, Colorado Springs, CO 80903, USA
[b] Department of Earth and Planetary Sciences, Washington University, St. Louis, MO 63130, USA
[c] Department of Geosciences, University of Arizona, Tucson, AZ 85721, USA

ARTICLE INFO

Article history:
Received 21 October 2014
Received in revised form 26 February 2015
Accepted 3 March 2015
Available online 14 March 2015

Keywords:
Devonian
Mississippian
Detrital zircons
Chemostratigraphy
Montana
Utah

ABSTRACT

Upper Devonian to Lower Mississippian strata in Utah and Montana record global events through this important interval in Earth history. Late Famennian strata of the Beirdneau, Leatham, and Pilot Shale formations in Utah, and Three Forks and Sappington formations in Montana, record widespread deposition of generally fine-grained siliciclastic and carbonate strata. Integration of sedimentology, physical stratigraphy, chemostratigraphy, and published biostratigraphy allows for the recognition of important disconformities and regional stratigraphic patterns. These enable the reconstruction of uppermost Devonian to lowermost Mississippian depositional, tectonic, and eustatic history of the region.

Carbon isotopic data allows for stratigraphic evaluation of the presence and absence of global bioevents of the Late Devonian, including the Annulata, Dasberg, and Hangenberg events, some of which are clearly recorded in hinterland deposits to the east in Colorado. While the Devonian–Mississippian boundary is also missing in our sections, a significant positive shift in $\delta^{13}C_{carb}$ in Lower Mississippian strata in Utah and Montana represents one of the largest positive $\delta^{13}C_{carb}$ isotope excursions of the Phanerozoic, linked to drawdown of atmospheric CO_2 and glaciation in the Kinderhookian.

Detrital zircon spectra from latest Devonian to Early Mississippian strata of Utah and Colorado include populations representing derivation from the Mazatzal and Yavapai provinces, Middle Proterozoic anorogenic granite bodies, and a small influx of Grenville and presumed Appalachian–Caledonian grains. Minor Paleoproterozoic and Late Archean peaks in Utah are likely multiple generation grains originally derived from the Peace River Arch of northwestern Canada and recycled in Ordovician rocks of Nevada. These patterns in detrital zircon geochronological data reflect, in part, changes in sediment dispersal patterns due to tectonic and eustastic variability within the Antler foreland basin during the Devonian–Mississippian boundary interval. This variability also led to irregular spatial patterns of unconformity development, as well as complicated physical stratigraphic and chemostratigraphic architecture.

1. Introduction

Major changes to the hydrosphere, atmosphere, and biosphere during the Late Devonian to Early Mississippian include the onset of glaciation, large eustatic sea level fluctuations, and changes to biogeochemical cycling (Walliser, 1984; Johnson et al., 1985; Streel et al., 2000; Joachimski and Buggisch, 2002; Sandberg et al., 2002; Brand et al., 2004; Buggisch and Joachimski, 2006; Cramer et al., 2008; Kaiser et al., 2008; Myrow et al., 2011, 2013). Changing tectonics, coupled with a terrestrial plant radiation (Algeo et al., 1995; Algeo and Scheckler, 1998; Caplan and Bustin, 1999; Streel et al., 2000; Algeo, 2004) led to global climatic cooling and the initiation of glaciation in the southern hemisphere (Streel et al., 2000; Raymond and Metz, 2004; Caputo et al., 2008; Brezinski et al., 2010; Wicander et al., 2011).

A long-term major sea level fall (Caputo and Crowell, 1985; Isaacson et al., 1999, 2008; Streel et al., 2000; Sandberg et al., 2002) was punctuated by a series of glacial–interglacial events that were, in cases, linked to major and minor perturbations to the biosphere, including mass extinctions. The well-known Frasnian–Famennian mass extinction (Kellwasser Event) (House, 2002; Kaufmann et al., 2004; Stigall, 2012) was one of many important biotic events that followed in the Famennian. These events were linked to global transgression, extensive

* Corresponding author at: Department of Geology and Geophysics, Yale University, New Haven, CT 06511, USA. Tel.: +1 719 389 6790; fax: +1 719 389 6910.
E-mail addresses: devon.cole@yale.edu (D. Cole), pmyrow@coloradocollege.edu (P.M. Myrow).
[1] Tel.: +1 719 389 6790; fax: +1 719 389 6910.

http://dx.doi.org/10.1016/j.palaeo.2015.03.014
0031-0182/

oceanic anoxia, and widespread deposition of organic rich black shale (Berry and Wilde, 1978; House, 1985; Becker, 1993; Walliser, 1996; Caplan and Bustin, 1999; Kump et al., 2005; Racki, 2005; Kaiser et al., 2008). The Annulata, Dasberg, and Hangenberg black shale beds (Marynowski et al., 2010; Racka et al., 2010) and associated biotic events were also linked to changes in the isotopic compositions of seawater (Kürschner et al., 1993; Brand et al., 2004; Saltzman, 2005; Buggisch and Joachimski, 2006; Kaiser et al., 2006; Cramer et al., 2008; Myrow et al., 2011, 2013).

Based on spectral analysis of lithological variations within fine-grained carbonate and shale successions of the Upper Devonian in the Holy Cross Mountain of Poland, De Vleeschouwer et al. (2013) identified orbitally forced, 405 ky and 100 ky eccentricity cycles in strata that host these shale beds. Recent geochronological analysis by Myrow et al. (2014) confirms De Vleeschouwer et al.'s (2013) estimates that the transgressive black shale units were short lived, and potentially less than 50 ky, and thus consistent with an origin by glacio-eustasy. The Dasberg and Hangenberg events have either been correlated with regionally developed unconformities (Bless et al., 1993; Sandberg et al., 2002) and associated meteoric diagenetic alteration along these surfaces during regression, or in other cases documented in strata in western Laurentia (Myrow et al., 2011, 2013) by a large global rise in marine $\delta^{13}C$ values (Hangenberg Event) during subsequent transgression (Brand et al., 2004; Saltzman, 2005; Buggisch and Joachimski, 2006; Kaiser et al., 2006, 2008; Cramer et al., 2008).

Another large positive carbon isotope excursion has been recognized globally in middle Tournaisian (Kinderhookian) carbonate strata of the Upper *crenulata* (*Siphonodella isosticha*) conodont zone. This excursion, which reaches a maximum value of >+7‰, has been documented in North America, Europe, and South China and Russia, and is one of the highest carbon isotope peaks of the Phanerozoic (Bruckschen and Veizer, 1997; Saltzman et al., 2000; Saltzman, 2002, 2003a,b; Katz et al., 2007; Qie et al., 2011). The rise of vascular land plants, changes in paleogeography, and regional tectonic events (e.g., Antler orogeny), are considered the impetus for decreased atmospheric CO_2, increased burial of organic material, and concomitant glaciation, all of which are associated with the distinct positive isotopic anomaly (Berner, 1990; Algeo and Scheckler, 1998; Mii et al., 1999; Saltzman et al., 2000; Qie et al., 2011). In North America, this excursion has been identified at strata in Nevada, Utah, Wyoming, and Idaho with isotope values consistently reaching +6–7‰ (Budai et al., 1987; Saltzman et al., 2000; Saltzman, 2002, 2003b; Gill et al., 2007). In this study we present the first high-resolution inorganic carbon isotope curves for these intervals from outcrops in Utah and Montana (Fig. 1) with accompanying detrital zircon data from four Upper Devonian sandstone samples in Utah and Colorado. These data are biostratigraphically constrained by published conodont data (Fig. 2).

This study explores the depositional history, geochemical signature, and detrital zircon geochronology of upper Famennian and Lower Mississippian strata from Utah and Montana (Fig. 2) in order to understand the record of events during this critical interval in western Laurentia. We emphasize the correlation of a series of regional unconformities and global bioevents in this unique interval of correlative strata stretching from Alberta to Nevada.

2. Location

We present data for uppermost Devonian and Lower Mississippian strata exposed in Utah and Montana (Figs. 1, 2). Upper Famennian strata of the Beirdneau and Leatham Formation in Leatham Hollow (LHU) are exposed southeast of Logan, UT (N041°38.871, W111°42.824, elevation 1966 m) (Fig. 3). Exposures of roughly coeval strata of the Pilot Shale outcrop at Little-Mile-and-a-Half Canyon (LMH) in the Confusion Range, Millard Co, UT (N039°13.041, W113°40.124, elevation 1972 m). A section of the Three Forks and Sappington formations was also measured along the flank of Peak 9559, next to Sacagawea Peak (SSM) in the Bridger Range ~25 km north/northeast of Bozeman, MT; access is through a steep valley just south of the Fairy Lake campground (N45°54′16.5″, W110°58′35.6″, 2893 m elevation). Finally, a section was measured along Beaver Creek (BCM), 35 km northeast of Helena, MT on a steep cliff north of the road (N46°50′33.5″, W111°45′16.9″, 1530 m elevation).

3. Field and laboratory methods

We measured and collected samples through ~135 m of the Pilot Shale at LMH (Fig. 4), and collected additional samples through 50 m of the overlying Joana Formation at this site. Samples for carbonate carbon isotope analysis were taken every ~25 cm through the entire section. At LHU, ~45 m of the Beirdneau and Leatham Formations were measured (Fig. 5), and samples were taken every ~10 cm throughout the section for carbonate carbon isotopes. At SSM, samples were taken every ~25 cm through ~90 m of the upper Trident Member of the Three Forks Formation, the Sappington Formation and the Lodgepole Limestone (Fig. 6). At BCM the uppermost 8 m of the Sappington formation was sampled every ~25 cm.

Approximately 550 carbonate carbon samples were drilled to powder using a dental drill. Approximately 150 μg samples of drilled carbonate powder were reacted with excess H_3PO_4 in He-flushed sealed tubes. Released CO_2 was then sampled using a Finnigan Gas Bench II, and isotope ratios were measured with a Delta V Plus Mass Spectrometer. Measurements are reported relative to the Vienna Pee Dee Belemnite (VPDB) standard using in-house standards calibrated with LSVEC, NBS-18 and NBS-19. Typical analytical errors were <0.1‰ (1σ) for $\delta^{13}C_{carb}$ and <0.2‰ (1σ) for $\delta^{18}O_{carb}$. All analytical data are reported in Data Repository 1.

Four sandstone samples were run for detrital zircon analysis. Three of these samples were processed, mounted, and analyzed at Arizona Laserchron Center using a Laser-Ablation Multicollector ICP Mass Spectrometer utilizing methods described by Gehrels et al. (2008). One sample (GCD-1) was analyzed by sensitive high-resolution ion microprobe (SHRIMP) at the Research School of Earth Sciences, Australian National University following procedures given in Williams (1998, and references therein). Data from the two labs are comparable in precision, with average uncertainties of 1.3% (SIMS) and 1.2% (LA-ICPMS) for 206/238 ages and 1.5% (SIMS) and 1.4% (LA-ICPMS) for 206/207 ages (all at 1-sigma). Analyses from both methods have been filtered using the same cutoffs of 10% for uncertainty of 206/238 and 206/207 ages, 20% reverse discordance, and 5% discordance. All analytical data are reported in Data Repository 2, along with Pb/U concordia and probability density plots for each sample.

4. Geologic setting

The tropically to sub-tropically positioned Laurentian continent was partially submerged in the Late Devonian, with expansive epicontinental seaways (Scotese, 2001). The upper Famennian strata of this study were deposited in a backbulge basin formed by the Antler orogeny. The Antler orogenic belt extended ~2300 km, from southern California, across Nevada and Idaho, and into Canada. The orogeny was the result of the eastward thrust emplacement of the Roberts Mountain allochthon, about 140 km east of its original position, beginning in the Late Devonian (Nilsen and Stewart, 1980). The thrust emplacement of the allochthon produced flexural warping of the North American craton, as modeled by Speed and Sleep (1982). This deformation produced a foreland basin, an upwarped forebulge, and a second wide, relatively shallow downwarped backbulge basin. The outcrops described herein deposited in the backbulge basin, which experienced flexural subsidence that created accommodation space for these Famennian strata. Relative sea-level falls and associated loss of accommodation space occurred during upwarping. It is likely that the uplifted forebulge created a barrier for the circulation of the epicontinental seaway filling

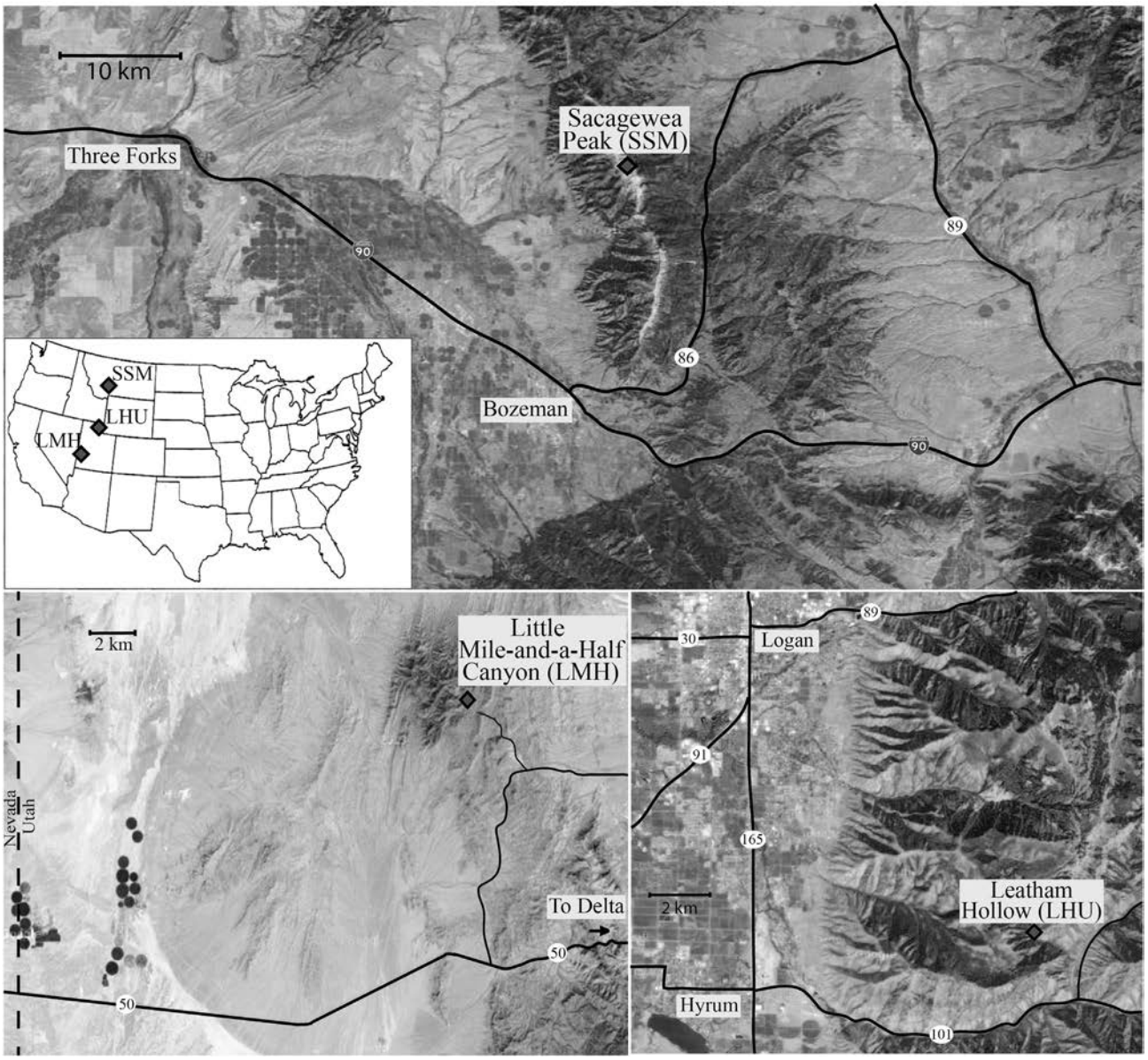

Fig. 1. Location map for Little Mile-and-a-Half Canyon, UT (LMH); Leatham Hollow, UT (LHU); and Sacajewea Peak, MY (SSM) sites.

the backbulge basin (Goebel, 1991; Giles and Dickinson, 1995). This had the most marked effect during periods of low sea level, and could have caused stratification of the basin, which has been suspected from sedimentological characteristics of certain restricted lithofacies (Goebel, 1991; Giles and Dickinson, 1995). Due to the presence of the migratory forebulge, it is likely that transgressions observed in syn-tectonic strata are the result of a combination of both eustatic and regional tectonic effects, which remain difficult to untangle (Saltzman et al., 2000).

5. Facies descriptions

5.1. Lower Pilot Shale

At Little Mile-and-a-Half Canyon (LMH), we measured 36.8 m in the upper part of the ~240 m thick lower Pilot Shale, a slope-forming unit characterized by tan weathering, gray 0.5–1.0 cm thick beds of calcareous siltstone. This part of the lower Pilot is assigned to the Lower and Upper *marginifera* conodont Zone, and represents the oldest strata in this study (Sandberg et al., 1980). A few unsorted, matrix-supported conglomerate units in the lower part of the formation are up to 3.7 m thick and represent debris flow deposits. The siltstone of the lower Pilot generally becomes more calcareous upsection, with thin grainstone and carbonate mudstone beds. At 31.65 m, there are 40 cm of yellow weathering, stacked, 0.3–1.5 cm thick grainstone beds with ripple scale cross-lamination and small scours. Additional features include bioturbated beds (e.g., at 24.17 m), slump intervals with ball-and-pillow structures (35.37 m), and reports of sole markings and bioclastic debris (Gutschick and Rodriguez, 1979). The upper part of the lower Pilot Shale is a 27.6 m of covered interval directly below the middle Pilot Shale (Fig. 4).

5.2. Beirdneau Formation and Trident Member of the Three Forks Formation

The <330 m thick, Famennian Beirdneau Formation consists of dolostone and quartz rich sandy dolostone, and sandstone (Sandberg and Poole, 1977; Sandberg et al., 1988). A resistant dolostone unit at the top of the formation, the “contact ledge” of Williams (1948),

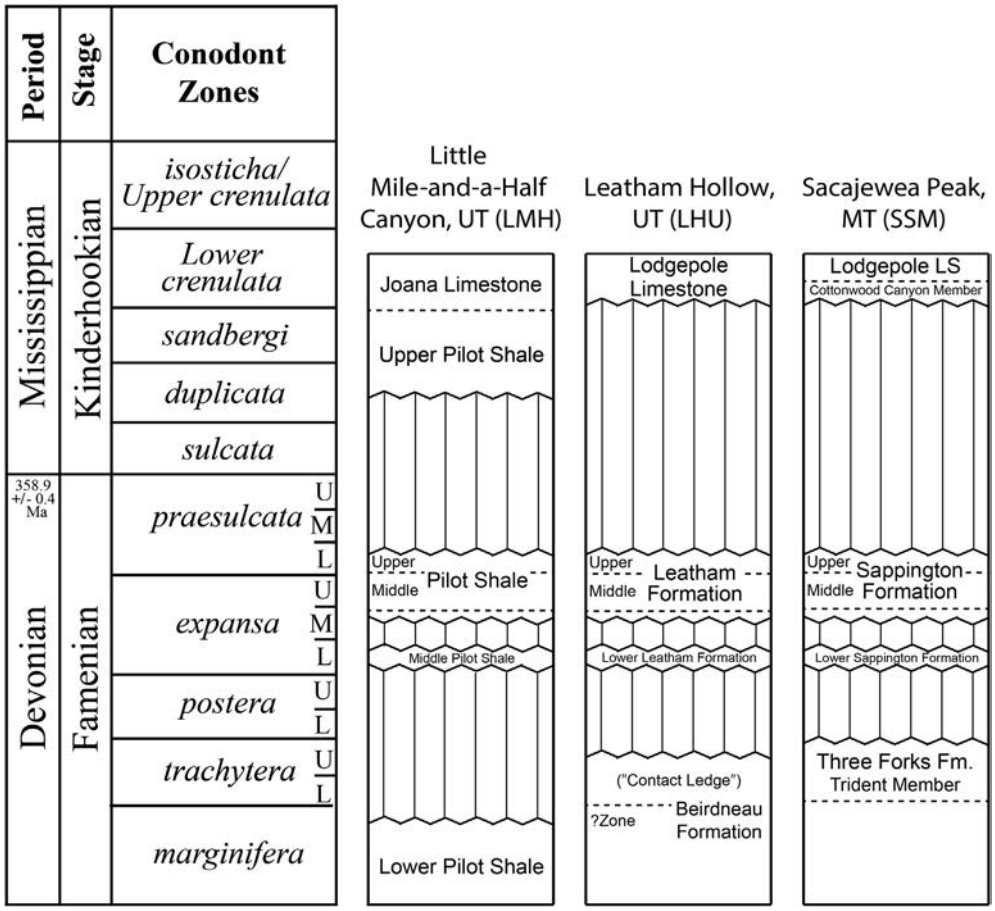

Fig. 2. Standard Upper Devonian Conodont Zones after Sandberg et al. (2002) on left. Date for base of Mississippian from Gradstein et al. (2012). Chronostratigraphic–lithostratigraphic framework for the strata of this study on right.

is 15 m thick at LHU and it forms the base of our section in this study (Fig. 5). The top 7 m of this unit is assigned to the Lower and Upper *trachytera* Conodont Zones, and the lower 8 m is unzoned (Sandberg and Gutschick, 1979). The lowermost 5.4 m is comprised of light blue to yellow weathering, finely laminated mudstone with 15–100 cm thick bedsets and 1–3 cm recessive breaks. Above this is 2.66 m of light gray fine grainstone with 3–25 cm thick beds at the base and thicker beds above. Above 8.06 m, there is 2.33 m of thin to thick-bedded massive and nodular mudstone, which locally contains abundant brachiopods. Above, there is 1.4 m of dark gray, brown weathering calcareous shaley siltstone beds with irregular micritic nodules, the top part of which contains abundant nodules that in cases form nearly continuous beds. This is overlain by 32 cm of dark gray irregular mudstone beds, then 51 cm of light gray, fossiliferous, fine grainstone. Above is a 22 cm thick partially silica-replaced, laterally linked, low-domal stromatolite bed. The formation is capped by 1.17 m of light gray, nodular weathering fossiliferous mudstone, 1.09 m of cover, and 12 cm of fissile gray shale at the contact with the Leatham Formation (Fig. 5), which is marked by a 3–7 cm thick medium to coarse sandstone bed.

The section at Peak 9559 in the Bridger Range of Montana (section SSM) exposes just over 24 m of roughly age-equivalent strata of the Trident Member of the Three Forks Formation (Fig. 6). The lowermost 98 cm consists of gray mudstone, fine grainstone, and very coarse grainstone. This is overlain by 5.18 m of thin bedded (5–10 cm thick), finely laminated, massive weathering, dark gray mudstone. This is followed by 11.7 m of cover, 3.85 m of flaggy weathering fine dolograinstone, 2.9 m of cover, and finally 65 cm of yellow weathering, gray, coarse grainstone. The strata have yielded conodonts of the *trachytera* Zone (Sandberg et al., 1988).

5.3. Lower parts of Leatham Formation and middle Pilot Shale, lower Sappington Formation

The Leatham Formation, exposed at LHU (Fig. 5), is the stratigraphic equivalent of the middle Pilot Shale at LMH (Fig. 4) (Sandberg and Poole, 1977; Sandberg and Gutschick, 1978; Gutschick and Rodriguez, 1979), and the lower Sappington Formation at SSM (Figs. 5, 7A) (Gutschick et al., 1962; Gutschick, 1964; Sandberg and Klapper, 1967). These strata are assigned to the Lower *expansa* conodont Zone. The base of these units are defined by a very thin basal sandstone and overlying black shale-rich deposits (Sandberg and Gutschick, 1969). At LMH we failed to locate the very thin sandstone bed at the base. Our section begins with 1 m of gray calcareous shaley siltstone. This is overlain 1.65 m of slightly silty, black fissile shale then 60 of covered interval. This is followed by 1.72 m of red-brown weathering tabular, interbedded siltstone, very fine sandstone, and fissile black shale. The siltstone and sandstone beds are up to 10 cm thick and rich with black-weathering chert. The cherty unit is overlain by 98 cm of chert-free, red-brown weathering interbedded siltstone, shaley siltstone, and very fine sandstone, which caps the lower part of the middle Pilot Shale.

At LHU (Fig. 5), a 3–7 cm thick medium-coarse grained, poorly sorted, calcareous sandstone bed at the base of the lower Leatham formation rests directly on the Beirdneau Formation at 15.32 m (Fig. 3). Above the sandstone lies 13 cm of light gray, brown weathering, calcareous siltstone, topped by 65 cm of light gray, thinly bedded fine grainstone. This is followed by an ~8 m thick dominantly covered interval with 1.10 m of poorly exposed, very thinly bedded (1–2 cm) calcareous siltstone and interbedded silty shale with black chert bands at 21.63 m. This corresponds to the cherty unit at LMH.

Fig. 3. Section at Leatham Hollow, UT, southeast of Logan, UT (N041°38.871, W111°42.824, elevation 1966 m), which exposes the Upper Devonian Beirdneau and Leatham formations, and the Lower Mississippian Lodgepole Limestone.

At SSM (Fig. 6), the correlative "lower black shale" of the Sappington Formation rests unconformably on a highly irregular erosional surface of the Trident Member of the Three Forks Formation below (Gutschick et al., 1962; Gutschick, 1964; Sandberg and Klapper, 1967). At SSM, this unit is represented by 2.15 m of black shale.

5.4. Middle Leatham Formation, upper part of Middle Pilot Shale, and middle part of Sappington Formation

A fine-scale detailed and spatially widespread lithostratigraphic framework exists for this particular interval (Gutschick and Rodriguez, 1979). A very thin (0 to 20 cm thick) discontinuous, poorly sorted, basal lag sandstone bed that locally contains fish bones, the prasinophyte alga *Tasmanites*, and *lumbricaria* traces (Gutschick and Rodriguez, 1979) mark the top of the underlying black-shale-dominated interval. Gradationally above lies a fissile, black spinicaudatan-rich shale bed up to 20 cm thick (ave ~10 cm), which is assigned to the Middle *expansa* conodont Zone. Spinicaudatans (clam shrimp), known by the paraphyletic term 'conchostracans', are weakly biomineralized, bivalved, extant branchiopod crustaceans. In Montana, a 10–15 cm thick green-gray shale with abundant bivalves, gastropods, brachiopods and pelmatozoan debris overlies this bed (Gutschick and Rodriguez, 1979; Sandberg et al., 1980); this unit is absent in other parts of western Laurentia. The rest of this stratigraphic interval consists of a complex (up to 5 m thick) carbonate deposit coined the "Oncolite-Shell-Sponge Bank Unit" (Figs. 8A, 9A, B) by Gutschick and Rodriguez (1979), which is assigned to the Upper *expansa* conodont zone, although the uppermost beds of this interval in two locations in Utah have yielded a Lower *praesulcata* conodont fauna (Sandberg et al., 1988).

At LMH (Fig. 4), the basal part of the oncolite-bearing unit is a 62 cm thick interval of grainstone with locally abundant bioclasts and irregularly shaped (non-spherical) oncolites and concretionary nodules, interbedded with shaley carbonate mudstone with irregular carbonate nodules. The next 2.75 m consist of interbedded carbonate mudstone to wackestone with disperse irregular nodules (20–50 cm thick beds) and bioclasts, and interbeds of fine grainstone (5–30 cm beds). This upper zone contains numerous fossils, including diverse brachiopods, bryozoans, calcareous sponges, goniatite cephalopods, mollusks, and a variety of trace fossils (Gutschick and Rodriguez, 1979).

At the base of this stratigraphic interval at LHU (Figs. 5, 9A, B) lies a 10 cm thick bed of black calcareous shale, topped by 12 cm of black carbonate mudstone with sparse spinicaudatan fossils. The basal black shale bed may correspond to the thin spinicaudatan-rich black shale unit described above but we did not recover any fossils from it, or find a thin underlying sandstone bed. The base of the "oncolite-bearing" carbonate unit consists of a 25 cm thick gray, coarse, crinoidal grainstone. The rest of this unit consists of 3.41 m of slightly fissile, light gray, thick bedded (42–80 cm), slightly shaley carbonate mudstone with irregular to flattened carbonate nodules. The beds at this locality lack the large oncolites present elsewhere.

At SSM (Fig. 6), the base of this interval is marked by 1 to 2 cm of indurated black shale with brachiopods and spinicaudatans. The overlying 1.62 m is composed of yellow weathering, mottled gray, fine grainstone with abundant bioclast of crinoids and brachiopods, as well as oncolites up to 5 cm in diameter.

5.5. Upper Leatham Formation, Upper Pilot Shale, and upper Sappington Formation

The upper Pilot Shale is a slope forming, poorly exposed unit that is lithologically similar to the lower Pilot Shale with respect to lithology and a general absence of fossils. The base of this unit is commonly gradational, although at LMH (Fig. 4) channel-fills of mudstone and coarse sandstone have been reported cutting down into the oncolite bank unit (Gutschick and Rodriguez, 1979; Sandberg et al., 1980). The upper Pilot consists primarily of interbedded, tan weathering, calcareous siltstone and silty shale, with intermittent beds of fine to very fine silty grainstone (Fig. 9A). Grainstone beds 5 to 16 cm thick are carbonate cemented, partly concretioned, and most abundant between 80 and 87 m. The siltstone and silty shale interbeds range from 2 to 10 cm thick. A few massive beds of dolomitic siltstone are up to 82 cm thick. At LMH, the lower part of the upper Pilot Shale is assigned to the Lower *praesulcata* Zone, but an unconformity at ~90 m in the section

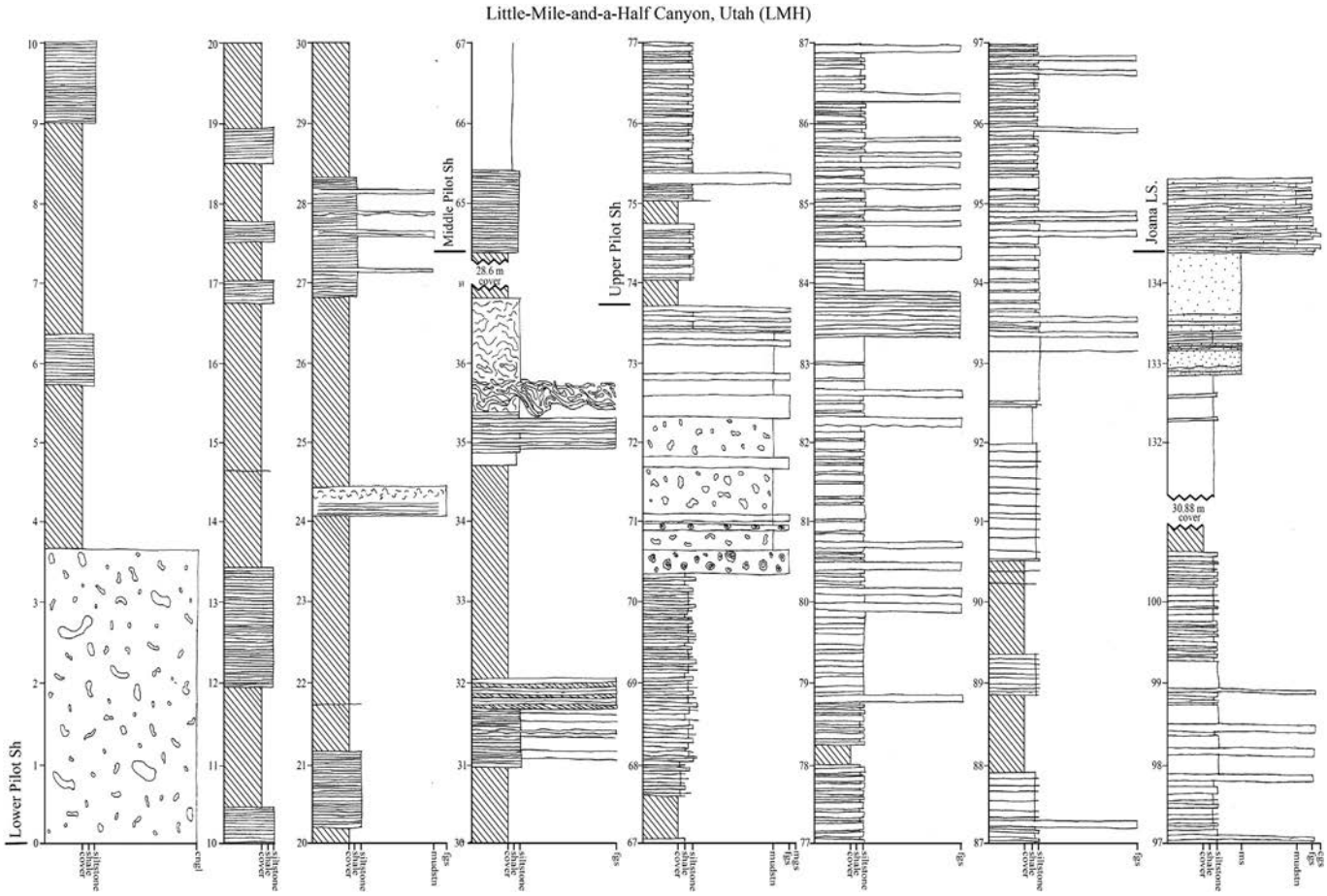

Fig. 4. Detailed stratigraphic section for Little Mile-and-a-Half Canyon, UT (LMH). Mudst = carbonate mudstone, fgs = fine grainstone, mgs = medium grainstone, and cgs = coarse grainstone.

marks a transition to *duplicata* Zone strata (missing Middle and Upper *praesulcata* and entire *sulcata* Zone). This unconformity thus marks the Upper Devonian–Lower Mississippian boundary at this section. The uppermost part of the upper Pilot is assigned to the *sandbergi* Zone.

At LHU (Fig. 5), the lower 6 m of this unit, the upper Leatham Formation, contains black to brown weathering, marl and mudstone units of varying thicknesses (3–125 cm). Some of these units are flaggy weathered and contain silty breaks at 1 cm thick intervals. Sandberg and Gutschick (1969) mention the presence of trace fossils, brachiopods, and foraminifera in the unit. The top of this unit consists of 7.37 m of cover directly below the contact with the chert beds and limestone of the Mississippian Lodgepole Limestone.

The correlative upper Sappington Formation at SSM (Fig. 6) also consists dominantly of shale and siltstone, although it contains more sandstone in its upper part. Here, the unit is thought to be mostly Lower *praesulcata* Zone, although the lowermost part may be part of the Upper *expansa* Zone. At two localities in Montana the youngest part of this siltstone has Middle *praesulcata* conodont fauna (Sandberg et al., 1988). At SSM, a 13 cm massive gray mudstone caps the oncolite bank unit, followed by 1.18 m of yellow weathering, calcareous siltstone with 5–10% floating crinoid and brachiopod bioclasts. The next ~4.3 m are composed of yellow weathering, bioturbated, calcareous siltstone interbedded with ~1–8 cm thick fine sandstone beds with parallel and wave-ripple lamination. Above this lies 3.38 m of black shale with interbedded very thin siltstone and very fine sandstone beds (Fig. 8B). The final 6.44 m of the formation is yellow weathering, very thin to thick (2–82 cm), very-fine to fine sandstone, with widely-spaced siltstone and shale interbeds. The sandstone beds contain hummocky cross stratification, wave ripple cross stratification, and parallel lamination.

5.6. Basal Joana Limestone

The contact between the upper Pilot Shale and the Mississippian Joana Limestone at LMH (Figs. 4, 9) is an unconformity surface. An 11 cm thick bed of reddish-pink weathering, poorly sorted, carbonate cemented, medium sandstone overlies the unconformity surface. The top half of this bed is bioturbated. This bed is overlain by 1.2 m of medium sandstone with thin interbeds of calcareous siltstone. The top of the sandstone-rich interval marks a transition to interbedded dolomudstone and fine to coarse grainstone, typical of the Joana. The lowermost few meters of this unit are tentatively assigned to the *sandbergi* conodont Zone (Sandberg, 1979), while the next ~50 m are assigned to the *crenulata* Zone. The lower part of this ~50 m interval is confidently assigned to the Lower *crenulata* Zone and the rest represents the *isosticha*/Upper *crenulata* conodont Zone based on carbon isotope stratigraphy (see below).

5.7. Cottonwood Canyon Member of the Mississippian Lodgepole Limestone

The basal member of the Lodgepole Limestone unit, the Cottonwood Canyon Member, is exposed at (BCM) and SSM (Figs. 6, 8C and D), and has also been recognized as a thin (1.31 m) unit at the base of the

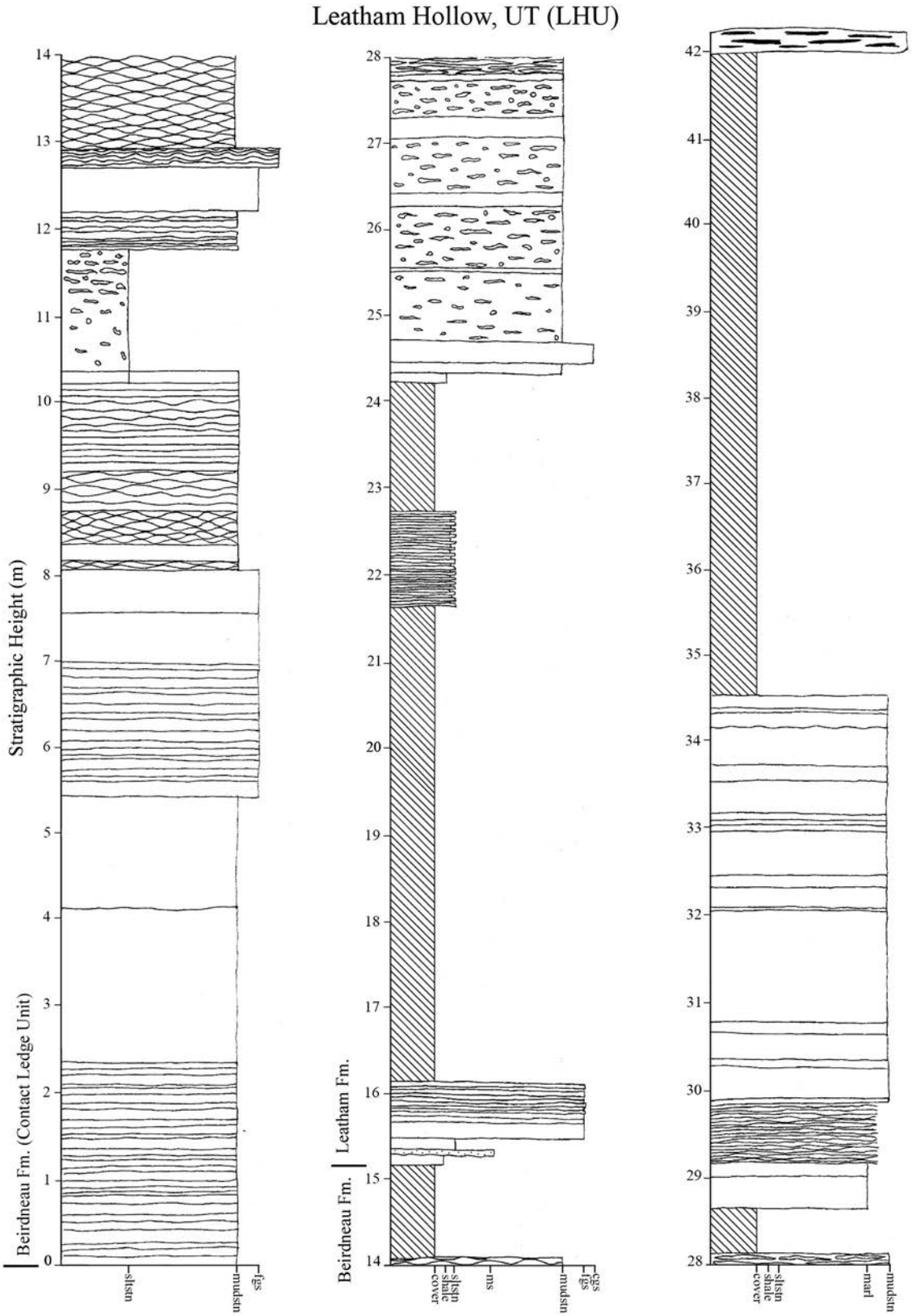

Fig. 5. Detailed stratigraphic section for Leatham Hollow, UT (LHU). Sltstn = siltstone, ms = medium sandstone, mudst = carbonate mudstone, fgs = fine grainstone, mgs = medium grainstone, and cgs = coarse grainstone.

Madison Limestone in Wyoming (Sandberg and Klapper, 1967). It is assigned to the Lower *crenulata* conodont Zone (Sandberg and Klapper, 1967). At SSM the member consists of an 83 cm thick basal layer of black, slightly silty, shale, which is overlain by 36 cm of shale and ~4 cm thick, brown calcareous fine sandstone and sandy grainstone beds (Fig. 8D). An 8 cm nodular limestone bed with silty breaks caps the member. The rest of the formation (Fig. 7B) consists of non-laminated thin-bedded lime mudstone, of which the basal beds

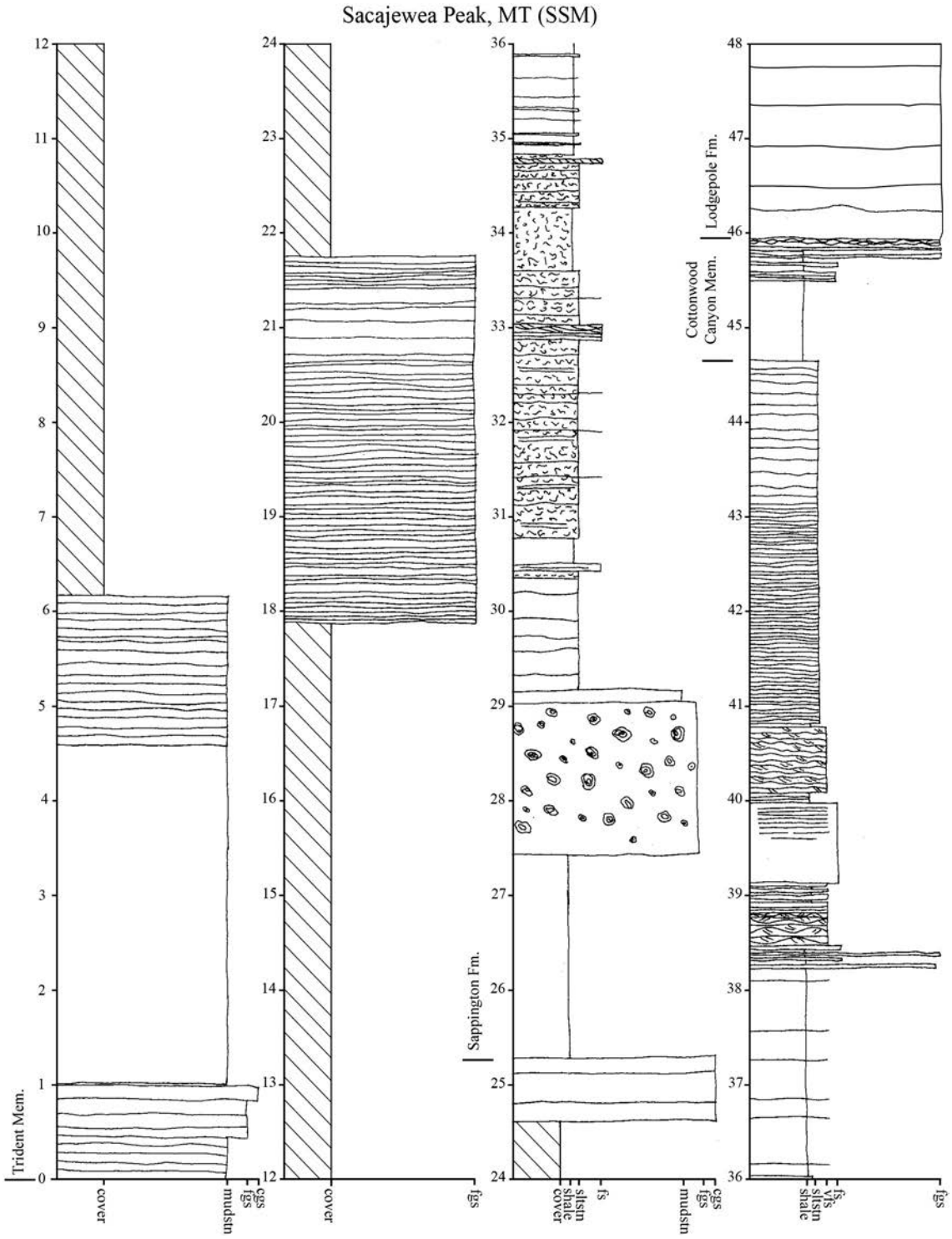

Fig. 6. Detailed stratigraphic section for Sacajewea Peak, MT (SSM). Sltstn = siltstone, mudst = carbonate mudstone, fs = fine sandstone, fgs = fine grainstone, and cgs = coarse grainstone.

assigned to the Lower *crenulata* Zone and the rest to the Upper *crenulata* Zone.

6. Facies interpretations

The general trend of upward increasing carbonate, including scoured and cross-stratified grainstone beds, suggests that the lower Pilot Shale records an overall regression. Slump deposits and unsorted, matrix-supported conglomerate beds, the latter interpreted to represent debrites, suggest unstable submarine slope conditions and abundant failures. Abundant ball-and-pillow structures are consistent with rapid deposition of sediment on water-lain mud, and are consistent with generally high accumulation rates. The thick covered interval at the top of the lower Pilot Shale precludes detailed interpretation of the transition to the middle Pilot.

The generally fine-grained lithologies of the 15 m thick unit at the top of the Beirdneau Formation at LHU suggest generally quiet water conditions. The presence of brachiopod fossils and stromatolites, and

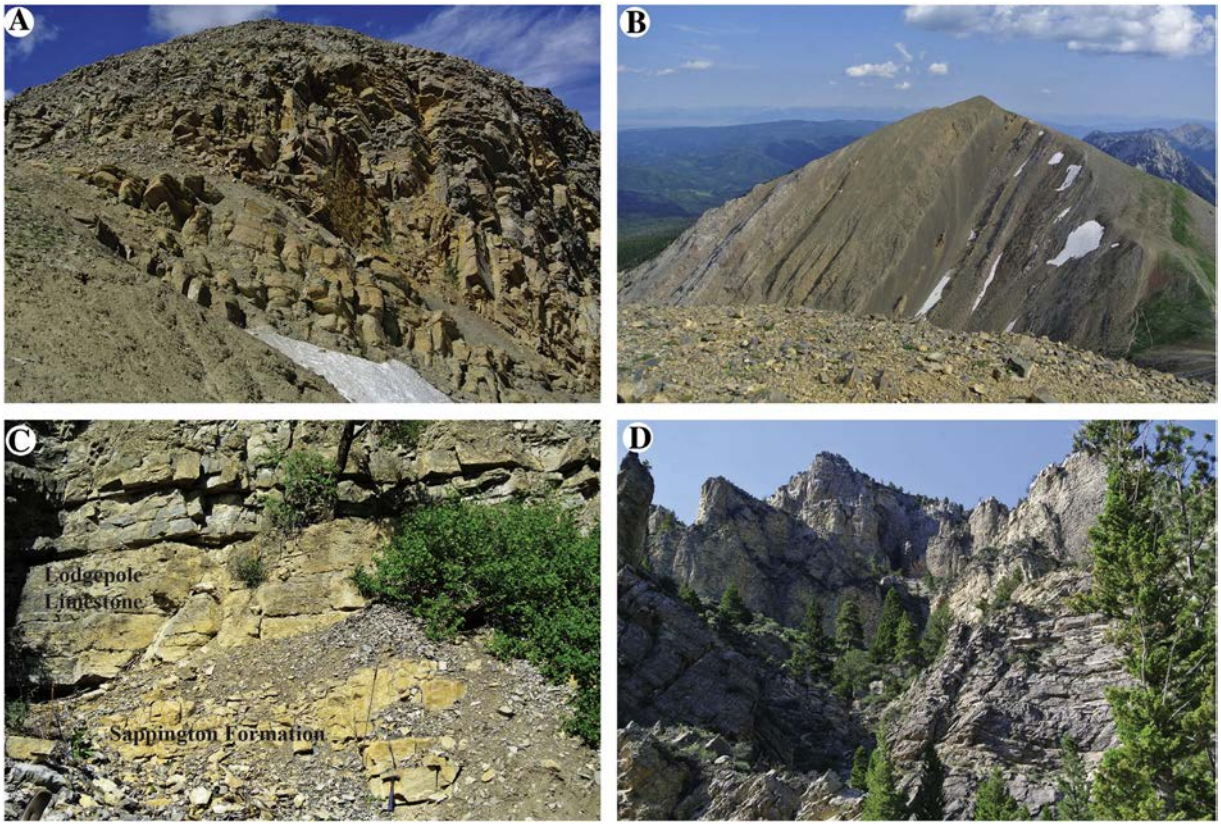

Fig. 7. Uppermost Devonian and Lower Mississippian strata in southwest Montana. (A) Upper Devonian Sappington Formation (foreground) and overlying Mississippian Lodgepole Limestone near Sacagawea Peak (SSM) in the Bridger Range near Bozeman, MT; (N45°54′16.5″, W110°58′35.6″, 2893 m elevation). (B) Thick Mississippian section of Lodgepole Limestone at SSM. (C) Sappington Formation–Lodgepole Limestone contact at Beaver Creek (BCM), 35 km northeast of Helena, MT (N46°50′33.5″, W111°45′16.9″, 1530 m elevation). (D) Lodgepole Limestone at BCM.

the abundance of lime mudstone and fine grainstone indicate marine deposition, and the intervals of shale and shaley siltstone indicate that deposition took place in a mixed siliciclastic–carbonate setting where fine grained silt and clay was deposited from suspension. The thin medium- to coarse-grained sandstone bed that marks the base of the overlying Leatham Formation is a significant sequence boundary that separates *trachytera* Zone strata from that of the Lower *expansa* Zone (missing *postera* Zone). The Trident Member of the Three Forks Formation at SSM is lithologically highly variable, including mudstone and both fine and coarse grainstone. The coarse grainstone suggests occasionally higher energy conditions than those recorded in the Beirdneau Formation. The equivalent sandstone bed and sequence boundary is not well exposed at SSM, although it is noted in adjacent areas within Montana (Sandberg and Poole, 1977; Sandberg and Gutschick, 1978; Gutschick and Rodriguez, 1979).

The lowermost Leatham, lower part of the middle Pilot, and the lower Sappington formations are all assigned to the Lower *expansa* conodont Zone. The sequence boundary at the bases of these units is highlighted by the highly irregular erosional surface at the top of the underlying Trident Member (Gutschick et al., 1962; Gutschick, 1964; Sandberg and Klapper, 1967). The thin basal sandstone beds that rest on this extensive surface is considered to be a thin transgressive lag deposit. Overlying finer grained deposits, such as the "lower black shale" of the Sappington Formation and black shale beds at LMH, represent further transgression and deposition locally of organic-rich mud in quiet, oxygen-poor conditions (Sandberg and Gutschick, 1969). Shallower water conditions are recorded above these shale beds at both LHU and LMH where a chert-rich interval is capped by heterolithic strata, including fine sandstone, and then another sequence boundary marked by another thin sandstone bed and overlying Middle *expansa* conodont Zone strata.

The remarkably widespread, fine-scaled stratigraphy of the middle Leatham, upper Middle Pilot, and middle Sappington formations (Gutschick and Rodriguez, 1979) reflects consistent depositional conditions over much of this part of western Laurentia at this time. The very thin to medium beds of sandstone at the bases of these units represent a widespread transgressive lag, which reworked fish bones and incorporated the prasinophyte alga *Tasmanites*. The overlying spinicaudatan-rich, ~10 cm thick, black shale indicates extremely shallow water conditions, given the ecological distribution of modern and ancient spinicaudatans (see discussion below).

The extinct spinicaudatan species present in this study, *Cyzicus lioestheria*, has been identified within this thin, yet remarkably extensive unit stretching from Alberta to Nevada (Gutschick and Rodriguez;, 1979; Sandberg et al., 1980). The majority of spinicaudatans, especially extant varieties, are known to live in small, often ephemeral, freshwater ponds, though there are certain species which are reported to inhabit a variety of brackish water environments (Tasch, 1977; Gutschick and Rodriguez, 1979; Webb, 1979; Vannier et al., 2003). In this study, the stratigraphic transition of the spinicaudatan-bearing shale and marl to overlying beds with marine fauna raises the possibility that the spinicaudatan shale was deposited in brackish environments, and that transgression led to preservation of normal marine fauna.

The organic rich black shale also likely represents oxygen poor conditions (Myrow, 1990). The typical open marine fossils of the overlying green-gray shale at SSM (Gutschick and Rodriguez, 1979; Sandberg et al., 1980) indicate transgression after deposition of

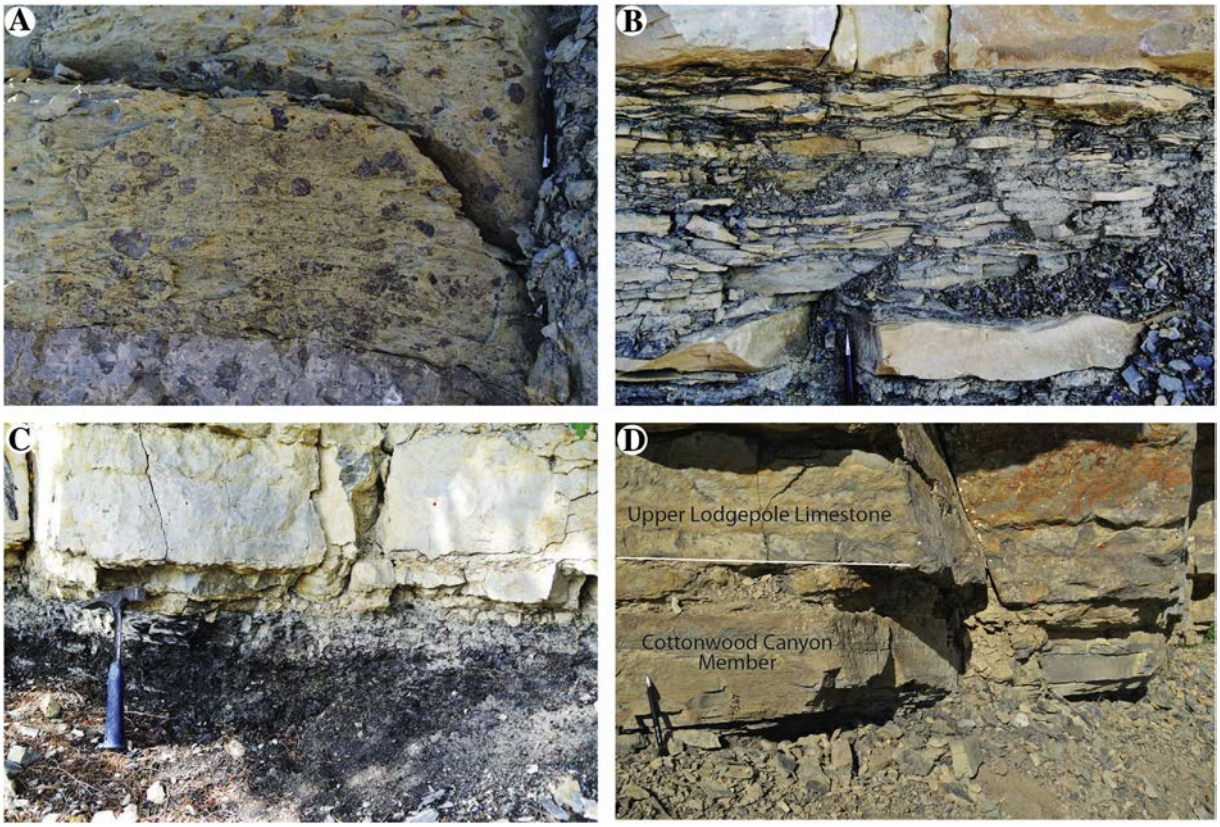

Fig. 8. (A) Unit rich in oncolites and concretionary nodules in middle Sappington Formation at location SSM. Note irregular shapes of the oncolites. (B) Lower part of upper Sappington Formation with irregular, thin wave-ripple laminated and hummocky cross-stratified fine sandstone and black shale. (C) Black shale of the Cottonwood Canyon Member of the Lodgepole Limestone and overlying limestone at BCM. (D) Contact between the recessive weathering uppermost Cottonwood Canyon Member and overlying member of the Lodgepole Limestone at the SSM section.

marginal marine facies. The Upper *expansa* to Lower *praesulcata* Zone oncolite-bearing unit with a wide variety of open-marine fossils (Gutschick and Rodriguez, 1979) represents a carbonate buildup that had clear relief on the sea floor. The coarse, locally crinoidal, grainstone at the base of the unit at LMH and the abundant oncolites indicate locally high-energy conditions. The fact that the oncolites are generally dispersed within carbonate mudstone suggests transport of the oncolites into a quiet-water setting adjacent to a high-energy environment that was capable of producing large oncolites (up to 5 cm diameter). Detailed interpretation of this unit is investigated in detail in Myrow et al. (in review).

The fine-grained, slope-forming upper Leatham, upper Pilot, and upper Sappington formations were deposited under similar conditions as those of the lower Pilot Shale. The contact with the underlying oncolite bank is generally gradational, although the channel-fills of mudstone and coarse sandstone that cut down into the oncolite bank (Gutschick and Rodriguez, 1979; Sandberg et al., 1980) may represent a relative sea-level drawdown, although it would have been a short-term event, given that there is no evidence for a biostratigraphic break. The calcareous siltstone and silty shale record mixing of fine-grained siliciclastic and carbonate sediment in a quiet water environment, and the very thin to thin interbeds of silty grainstone beds may represent distal tempestite deposits. Abundant and locally thick units of siltstone below the basal Mississippian unconformity, at ~90 m at LMH within the upper Pilot, may reflect shoaling up to a sequence boundary surface that records nondeposition or erosional removal of strata representing the Middle and Upper *praesulcata* Zone and entire *sulcata* Zone. Brachiopod and crinoid fossils, as well as bioturbation, in the upper Sappington Formation at SSM indicate a quiet water open marine depositional environment. Very thin to thin beds of fine sandstone with parallel and wave-ripple lamination are interpreted to represent relatively distal tempestites. Similar sedimentary structures, as well as hummocky cross stratification, in the very thin to thick sandstone layers in the uppermost 6.44 m of the formation, reflect high-energy storm deposition.

At LMH, the lowermost Mississippian Joana Limestone is an unconformity surface marked by overlying, poorly sorted, medium sandstone. The presence of *sandbergi* Zone strata below and above this surface (Sandberg, 1979) dates the timing of sea level drawdown and indicates a relatively short hiatus. The transition to dolomudstone and grainstone above is consistent with transgression above shoreline sandstone deposits. The base of the thin Cottonwood Canyon Member of the Lodgepole Limestone unit at SSM in contrast, represents a significant unconformity that has Lower *crenulata* Zone strata (Sandberg and Klapper, 1967) resting on *praesulcata* Zone strata. The silty shale and minor sandstone and grainstone beds lack any diagnostic sedimentary structures, thus their environments of deposition are difficult to interpret. The shift from mixed siliciclastic–carbonate strata of the Cottonwood Canyon member to overlying dominantly carbonate strata suggests initial input of siliciclastic sediment during the initial stages of transgression, and subsequent loss of input of terrestrial sediment by runoff during further relative sea level rise.

7. Carbon isotope chemostratigraphic results

The chemostratigraphic results of this study extend from middle Famennian (*marginifera*) to lower Mississippian (Upper *crenulata*). *Marginifera* Zone strata of the Lower Pilot Shale at LMH have $\delta^{13}C_{carb}$ values at the base that largely oscillate between 0 and −1‰ up to 23.32 m (Fig. 10). Above this, the values generally are more negative, but show substantial variation, with multiple oscillations between −0.5‰ and −5.0‰. The highly negative $\delta^{13}C_{carb}$ values in these

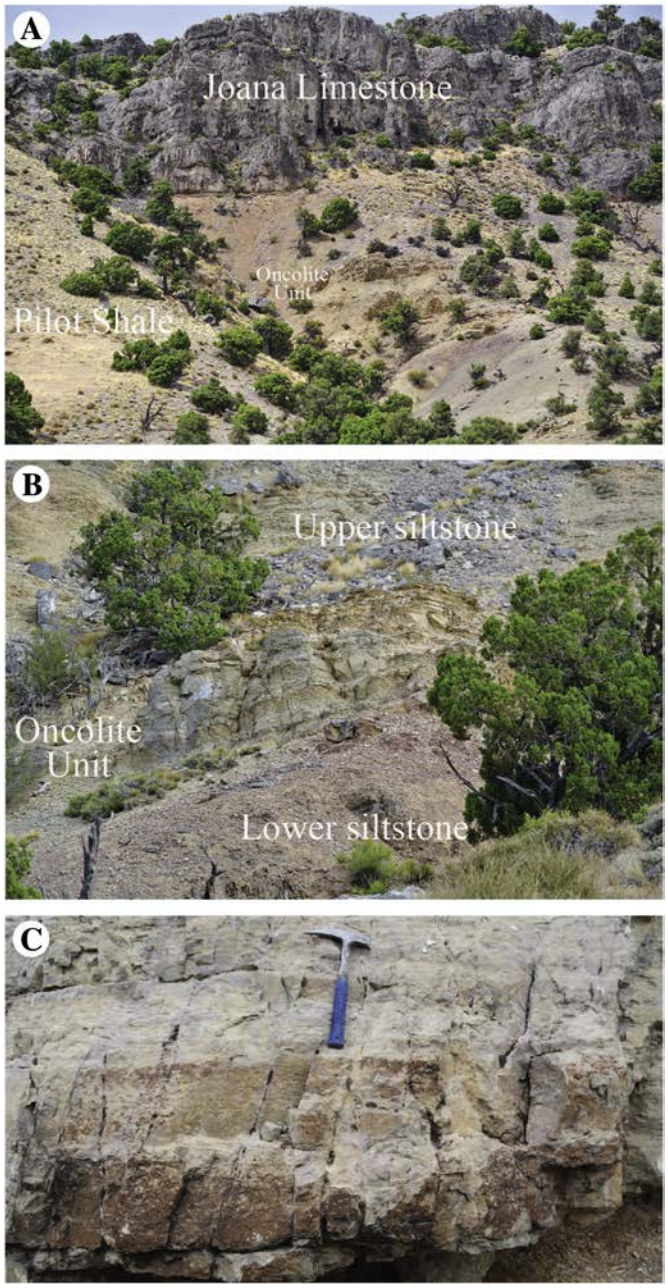

Fig. 9. (A) Pilot Shale and the cliff-forming Joana Limestone at Little Mile-and-a-Half Canyon, UT (LMH). (B) Oncolite-bearing wackestone of the lower Middle Pilot shale and both overlying and underlying siltstone deposits. (C) Sandstone bed at the base of the Joana at LMH.

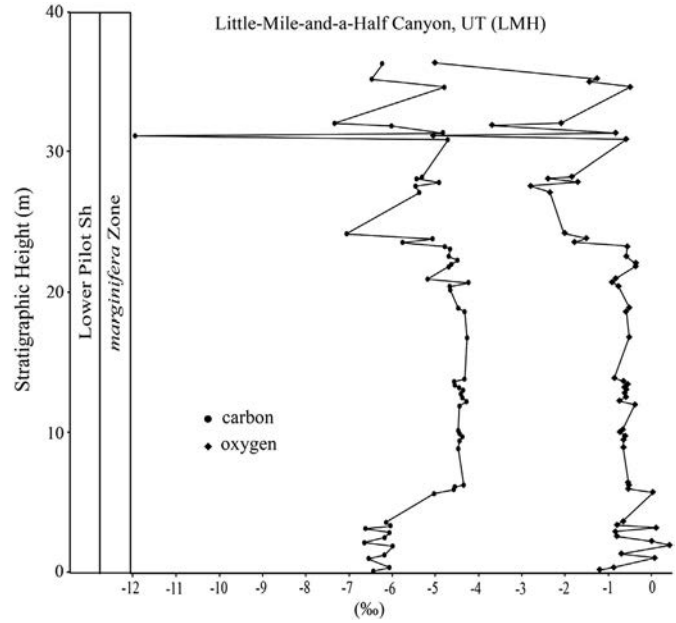

Fig. 10. $\delta^{13}C_{carb}$ and $\delta^{18}O$ data for *marginifera* Zone strata of the lower Pilot Shale at Little Mile-and-a-Half Canyon, UT (LMH).

oscillations coincide with beds of cross-laminated grainstone, small scours, and a slump zone with ball-and-pillow structures within isolated 1–2 m thick exposures through the primarily slope-forming and commonly covered section.

Trachytera age strata exposed at LHU and SSM (Figs. 11, 12) also yielded carbon isotopic data. At LHU, values at the base of the 15-m-thick Beirdneau Formation at LHU oscillate between ~−0.4‰ and ~0.5‰ up to 7.86 m. Above this level, there is a slight negative shift to values ~−1‰ up to 11.63 m. The rest of the formation shows significant variation in values, oscillating between −2.5‰ and 1.1‰ over this 3.69 m interval. At SSM, $\delta^{13}C_{carb}$ values in the lower part of our section of the Trident Member of the Three Forks Formation range between 0 and −2‰ with one exception of −4.0‰. Above an 11.7 m covered interval, between 17.98 and 21.73 m, $\delta^{13}C_{carb}$ values are tightly clustered between 0.0 and −0.1‰.

Our only $\delta^{13}C_{carb}$ data from the Lower *expansa* Zone are from the basal Sappington Formation at SSM directly above a 2.9 m covered interval at the top of the Trident Member (Fig. 11). The lowermost sample has a $\delta^{13}C_{carb}$ that is anomalously high (2.4‰), and above are three samples that average 0.7‰.

Carbon isotopic data for Upper *expansa* and Lower *praesulcata* strata are presented for the middle and lowermost upper Pilot Shale at LMH, the middle and upper Leatham Formation at LHU, and the middle and upper Sappington Formation at SSM (Figs. 11, 13). No lithologies were suitable for carbon isotope analysis in the lower black shale or the spinicaudatan interval in Utah (Lower to Middle *expansa* Zone), and thus the lowest samples of this interval there are from Upper *expansa* strata at the base of the oncolite-bearing carbonate unit (Fig. 13). The $\delta^{13}C_{carb}$ values in the basal ~4 m of this interval at LMH oscillate between 1.0 and 2.8‰ with the average drifting slightly negative from ~2.2 to ~1.3‰. A jump to more negative $\delta^{13}C_{carb}$ values at the base of the Lower *praesulcata* Zone is followed by consistent values of ~0.5‰ interspersed with more positive values between 0.9 and 1.7‰. These oscillations may be due to the presence of numerous nodules, which may not record true secular variations in the marine isotope record. The $\delta^{13}C_{carb}$ values at LHU (15.32 m–41.89 m) display similarly positive values and variation (1.5‰ to 3.9‰) through the oncolite unit, and a similar negative shift in the upper part of the Leatham Formation at the base of the Lower *praesulcata* Zone. At SSM, $\delta^{13}C_{carb}$ values in the 1.6 m thick oncolitic unit are ~2–3‰. Just above are two anomalous negative values close to −1‰, and then the next 10 m of strata have relatively uniform values between 2 and 3‰. The uppermost Lower *praesulcata* Zone strata have similar values that average ~2‰ but with scattered negative values that reach −1.0‰. At BCM, values also average ~2‰, but have little variability. There is a slight negative shift in values at the top of the section below the Lodgepole Formation.

Strata of the *Duplicata* and *sandbergi* zones, exposed in the middle and upper parts of the Upper Pilot Shale at LMH rest disconformably on Lower *praesulcata* Zone strata (missing Middle/Upper *praesulcata* and *sulcata* zones). The $\delta^{13}C_{carb}$ isotope values of these zones (Fig. 13) are the least variable of the Pilot Shale. They vary between 0.0 and 1.2‰, with the exception of one sample of 1.6‰. There is a slight

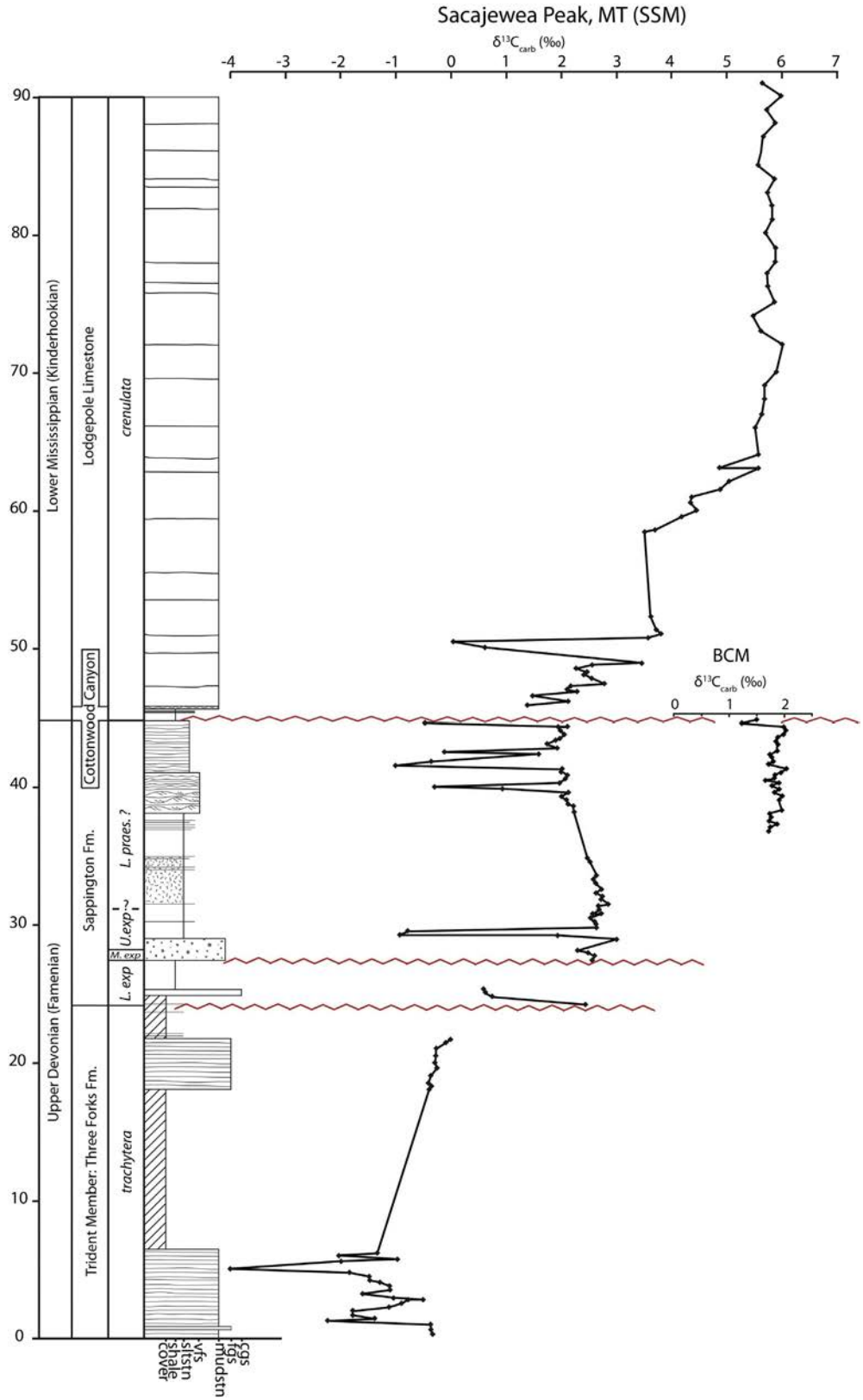

Fig. 11. $\delta^{13}C_{carb}$ data for uppermost Devonian strata at Sacajewea Peak, MT (SSM) and Beaver Creek (BCM).

positive drift in the lower 5 m of this interval, and the rest is remarkably uniform.

Strata of the Lower *crenulata* and Upper *crenulata*/*isosticha* conodont Zones are exposed at both LMH in the Joana Limestone (Fig. 13) and SSM in the Cottonwood Canyon and Paine Shale members of the Lodgepole Limestone (Fig. 11). At SSM the $\delta^{13}C_{carb}$ isotope values trend positively over the first ~17 m of this zone (45.87–63.00 m), increasing from an initial value of 1.4 to 5.6‰. The remaining ~28 m of the section maintain consistently heavy values oscillating between 5.5 and 6.0‰. At LMH $\delta^{13}C$ isotope values rise rapidly in the basal

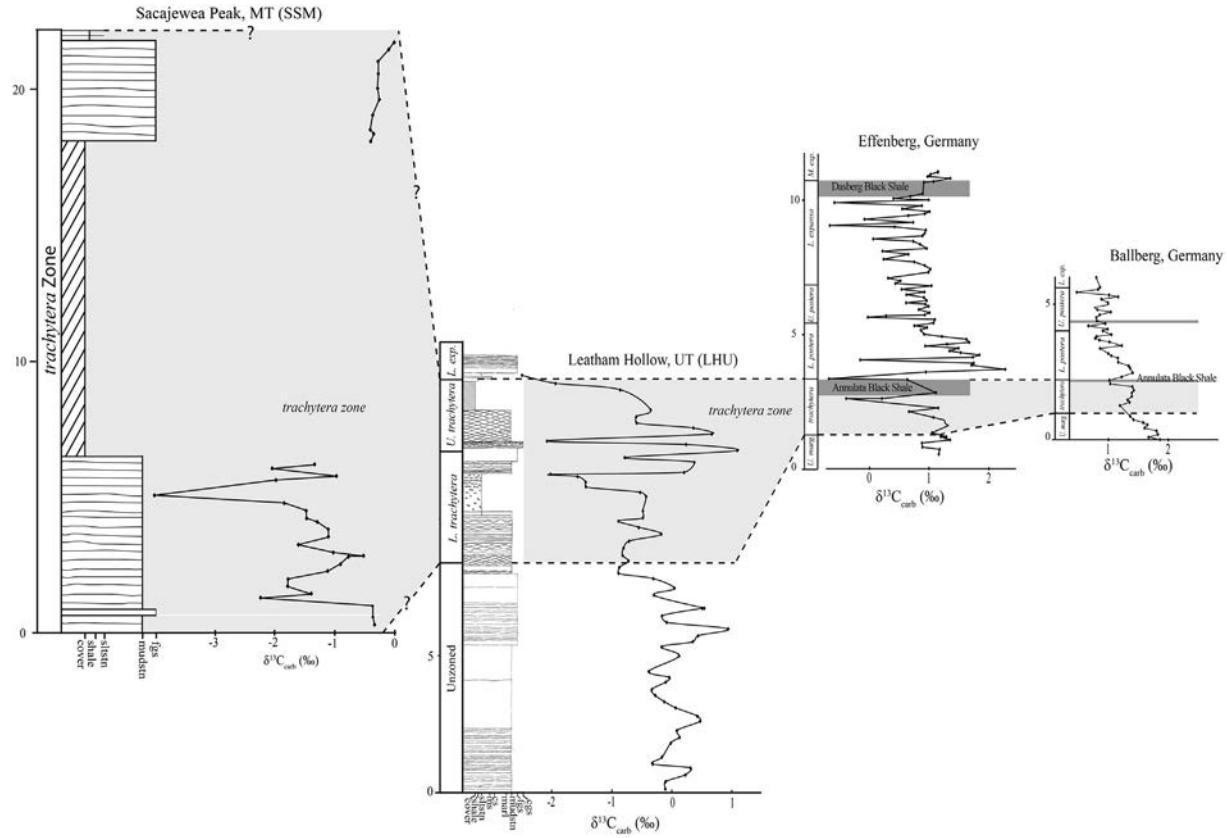

Fig. 12. $\delta^{13}C_{carb}$ data for *trachytera* Zone strata at Sacajewea Peak, MT (SSM); Leatham Hollow, UT (LHU); and two sections in Germany: Effenberg and Balberg. The German data are from Myrow et al. (2011; see for locations of sites).

~4.5 m (135.31–139.84 m) increasing from −0.3 to 2.3‰. Through the next ~22 m values trend positively and oscillate between 1.9 and 3.1‰, with the exception of one value of 0.8‰. The overlying ~13 m (161.9–174.40) are considerably more variable with values between 1.7 and 4.1‰. Samples were not collected through the following 6.4 m. In the topmost 5.4 m of the section, the heaviest values are present and range from 4.7 to 5.7‰.

We made plots of $\delta^{13}C$ versus $\delta^{18}O$ for the data derived from samples for each section described above (Data Repository 1) to test whether the samples were subjected to significant diagenetic alteration. In cases of strong diagenetic overprint, carbon and oxygen isotope values show statistically significant covariance. Linear regression r^2 values for the sections are as follows: LHU, 0.03; SSM, 0.32; LMH, 0.04; and BCM, 0.03. Thus, although SSM has a higher r^2 value, none of the sections show significant correlation and likelihood of alteration. LHU and LMH samples, which have uniformly high $\delta^{18}O$ values (almost entirely >−10‰), are almost certainly altered to a very small extent. Some SSM values are more negative (e.g., 5 values between −15 and −17‰), and these tend to be associated with decreased $\delta^{13}C_{carb}$ values; however, these samples give rise to isolated decreases in the $\delta^{13}C_{carb}$ signal that do not impact the overall stratigraphic pattern of the $\delta^{13}C$ record in SSM.

8. Interpretations: Carbon isotope chemostratigraphy

Below we interpret the $\delta^{13}C$ data from Utah and Montana in chronostratigraphic order from lower Famennian *marginifera* Zone to Mississippian *crenulata* Zone strata. Based on data from Sandberg et al. (1980), most of our data from the lower Pilot Shale at LMH can be assigned to the Lower *marginifera* Zone. The carbon isotopic data, which average ~−0.5‰ through the first 23 m, are ~2.0‰ lighter than published data from that zone in Germany, though fairly consistent. The data appear to lack any signal of the small positive carbon isotope excursion associated with the Enkeberg Event, an ammonoid extinction horizon and associated black shale unit (House, 1985; Becker, 1993). The uppermost 13 m are extremely variable, averaging ~4.0 to 5.0‰ lighter than data from Germany (Buggisch and Joachimski, 2006). The highly fluctuating and more negative overall values of our data reflect either local deviation from open marine $\delta^{13}C_{carb}$ values in these strata, consistent with the inferred brackish habitat for the spinicaudatan-rich strata (see Myrow et al., in review), or a greater impact of diagenetic alteration in these strata relative to those in Germany.

In Europe, latest *trachytera* Zone strata record the Annulata Event, the first of the well-known Famennian bioevents events with associated black shale beds (Becker, 1993; Sanz-Lopez et al., 1999; Becker and House, 2000; Sandberg et al., 2002; Korn, 2004; Hartenfels and Becker, 2009). This event was associated with global anoxia (Wilde and Berry, 1984; Walliser, 1996; Racka et al., 2010) and an interglacial sea level rise (Sandberg et al., 2002; Joachimski et al., 2009), but not a large perturbation of the biosphere or carbon cycle as with later events (Racka et al., 2010). The event included a radiation of the ammonoid *Platyclymenia annulata* (Walliser, 1984; House, 1985; Walliser, 1996), and muted changes in conodont fauna (Hartenfels and Becker, 2009). In Europe, it generally consists of two black shale beds with abundant ammonites, ostracods and bivalves (Korn, 2004).

In western North America, the Annulata Event roughly corresponds to transgressive deposits of Event 15 of Sandberg et al. (2002), including the Trident Member of the Three Forks Formation and the "contact ledge" of the Beirdneau Formation. These strata have only yielded conodonts from the *trachytera* Zone (Sandberg et al., 1988). However, latest *trachytera* Zone strata show little carbon isotopic variation, including the Annulata Event (Buggisch and Joachimski, 2006; Myrow et al., 2011). Thus, although there are stratigraphic changes to higher

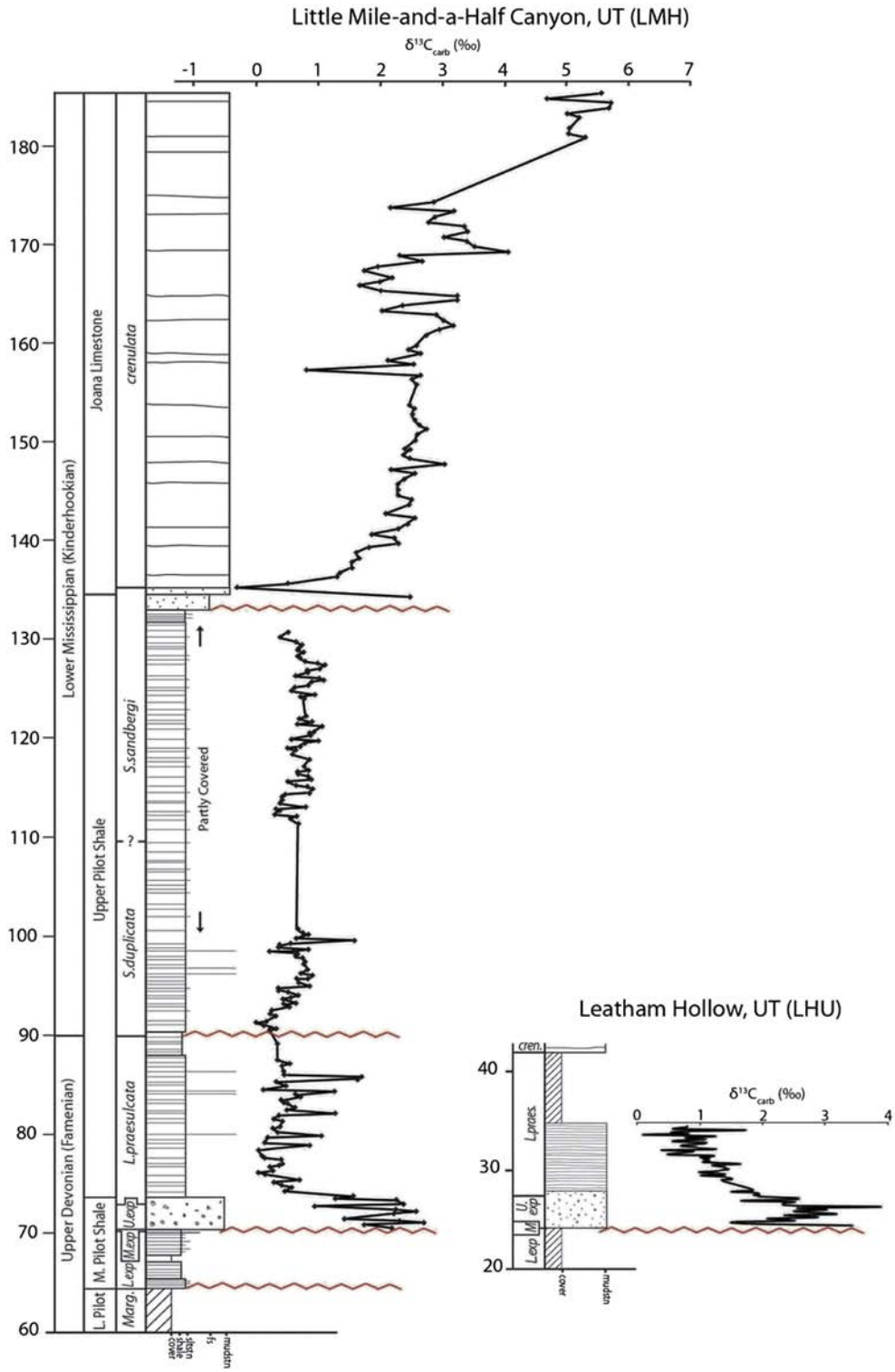

Fig. 13. $\delta^{13}C_{carb}$ data for youngest Upper Devonian strata at Little Mile-and-a-Half Canyon, UT (LMH) and Leatham Hollow, UT (LHU).

isotopic variability within the *trachytera* Zone strata at SSM and LHU (Figs. 11, 12), there are no definitive isotopic changes that can be directly linked to the Annulata Event in these sections.

The unconformity that marks the break between *trachytera* and Lower *expansa* Zone strata at SSM is located somewhere in the mostly covered interval between 21.73 m and 24.63 m (Fig. 6). The value from a thin carbonate bed at 24.24 m (2.5‰), and three overlying values from this interval that average ~0.7‰ (Fig. 11), are clearly more positive than the *marginifera* and *trachytera* values, and mark the beginning of a long term positive shift in values associated with late Famennian to Mississippian glaciation. The data are consistent with 1–2‰ values in strata of the upper part of the Lower *expansa* Zone (Myrow et al., 2011). The data are too sparse to allow detection of an isotopic signal of the Dasberg event, which is generally a low-amplitude excursion (Kaiser, 2005; Buggisch and Joachimski, 2006; Kaiser et al., 2008; Hartenfels and Becker, 2009; Myrow et al., 2011), and is located ~2/3 of the way through the Lower *expansa* Zone (Hartenfels and Becker, 2009). The transition from Lower *expansa* to Middle *expansa* zone at a

sandstone below the regionally extensive oncolite bed described herein is potentially related to the global Dasberg event, which in Europe consisted of a regression, development of an unconformity, and subsequent extensive transgressive deposition of Lower *expansa* Zone black shale (Becker, 1993; Sandberg et al., 2002; Kaiser et al., 2006; Hartenfels and Becker, 2009). The transition directly to Middle *expansa* Zone strata at the unconformity at the base of the sandstone, would suggest that the transgressive phase of the Dasberg is missing. This mirrors a similar stratigraphic relationship and unconformity in Morocco, produced in part by delayed onlap of Middle *expansa* Zone strata onto a basal Dasberg unconformity.

Very little $\delta^{13}C_{carb}$ isotope data are available for Upper *expansa* Zone strata globally. Buggisch and Joachimski (2006) present data for strata in central and southern Europe with a slight negative trend from the Upper *expansa* to Lower *praesulcata* zones, although the trend is difficult to precisely define due to few data points through this interval. Our LHU (26–28 m) and LMH (73–75 m) data (Fig. 13) show a similar negative drift, as well as similar absolute values that are generally close to 2.0‰. The 1.0‰ negative shift at the Upper *expansa*–*praesulcata* boundary at LMH may correlate to a similar shift in European strata (Kaiser et al., 2006), and the 1.5‰ and 2.0‰ $\delta^{13}C_{carb}$ values are in line with those documented through the Lower and Middle *praesulcata* (Buggisch and Joachimski, 2006; Kaiser et al., 2006). The *praesulcata* absolute values, however, are ~1.0‰ higher in the Kronhofgraben section (Carnic Alps) of Kaiser et al. (2006). $\delta^{13}C_{carb}$ values rise in the Middle to Upper *praesulcata* (Saltzman, 2005; Buggisch and Joachimski, 2006; Kaiser et al., 2006) reflecting the Hangenberg positive excursion. The Hangenberg excursion (Brand et al., 2004; Saltzman, 2005; Buggisch and Joachimski, 2006; Kaiser et al., 2006; Cramer et al., 2008; Myrow et al., 2011, 2013) lies just below the Devonian–Mississippian boundary in the Middle *praesulcata* conodont zone (Ziegler and Sandberg, 1984; Dreesen et al., 1988; Isaacson et al., 1999; Myrow et al., 2014), but strata of this age are absent in this study below unconformities due to nondeposition and/or removal.

Strata of the *duplicata* and *sandbergi* conodont Zones are represented in the Upper Pilot Shale at LMH. $\delta^{13}C_{carb}$ isotope values in this section (Fig. 13) rise from ~0.2‰ in the lowermost 5 m of the *duplicata* Zone, and then maintain remarkably consistent values around 0.8‰. Very little published isotopic data are available for these conodont zones, especially at a high enough resolution for comparison with this study. Kaiser et al. (2006) and Buggisch et al. (2008) present some data from Europe through these conodont zones, but values vary between 0‰ and +3‰ depending on the locality.

Strata of the *crenulata* Zone (primarily Upper *crenulata*), contains one of the largest positive $\delta^{13}C$ isotope excursions of the Phanerozoic (Budai et al., 1987; Bruckschen and Veizer, 1997; Saltzman et al., 2000; Saltzman, 2002, 2003b; Qie et al., 2011). This excursion has been documented globally to varying intensities (+4.2‰ in South China, ~+6‰ in Europe, and +7.5‰ in North America) in both bulk rock and brachiopod calcite, and is interpreted to reflect increased organic carbon burial (Bruckschen and Veizer, 1997; Mii et al., 1999; Saltzman et al., 2000; Saltzman, 2002; Gill et al., 2007; Katz et al., 2007; Qie et al., 2011). Saltzman et al. (2000) suggests a causal relationship between the rapid subsidence of the Antler foreland basin and the isotopic excursion. While it may be difficult to untangle regional tectonic effects from eustatic changes, the effects of the rise of vascular land plants, and continental drift, it is well established that the isotopic excursion is associated with drawdown of atmospheric CO_2 and glaciation in the Kinderhookian (Algeo and Scheckler, 1998; Saltzman et al., 2000; Saltzman, 2002; Saltzman et al., 2004). The Mississippian strata of the Lodgepole Formation, including units at SSM, have indicated that orbital-scale glacio-eustasy was in fact an important driver of oxygen isotopic changes (Wallace and Elrick, 2014), and presumably carbon isotopic variation as well.

Strata of the Lower *crenulata* Zone, represented by the Lodgepole limestone at SSM, were deposited during a rapid transgression (Sandberg et al., 1982). Based on the $\delta^{13}C$ isotope data of this study (Fig. 13), we assign the overlying conodont-barren strata at LMH, which comprise the bulk of the Joana Limestone (Sandberg, 1979), to the Upper *crenulata* Zone. The architecture of the $\delta^{13}C$ isotope curves at these localities is consistent with published data from the Joana Limestone of southeast Nevada and the Henderson Canyon formation of southeast Idaho (Saltzman et al., 2000; Saltzman, 2002). Both the SSM and LMH data sets (Figs. 11, 13) show a sharp increase in values at the base of the section, accompanied by increased variance with $\delta^{13}C_{carb}$ oscillating around ~2–3‰, and then higher values of ~+5–6‰. LMH only captures a short section of highly positive values. Saltzman et al. (2000) note that their section of the Joana Limestone from the Pahranagat Range is notably expanded ($\delta^{13}C_{carb}$ values only reach ~+3‰ in the first 50 m at this location, while at LMH, $\delta^{13}C_{carb}$ reaches +5.5‰ in 45 m of section). The data from SSM also show remarkable similarity to data of Saltzman (2003b) from Samaria Mountain in southeastern Idaho. Both sections show a rise in $\delta^{13}C_{carb}$ at the base of the section then a few significantly lighter data points before a rapid rise to consistently heavy values through ~20–30 m of section (Saltzman, 2003b, fig. 7). We cannot correlate the placement of the Lower *crenulata*–Upper *crenulata* boundary with a particular shift in the carbon isotope record due to the lack of high-resolution biostratigraphic data.

9. Detrital zircons: Results

Four detrital zircon sandstone samples from the western U.S. were analyzed during this study (Fig. 14), in part to understand how paleogeography and regional patterns of uplift, erosion, and deposition relate to the stratigraphic data and associated events recorded in the Devonian–Mississippian boundary interval strata described above. One sample (LHU-LF1) is from the lower sandstone of the Leatham Formation at LHU, which is assigned to the Middle *expansa* Zone. Another sample (LMH-132.92) is from the basal sandstone of the Joana Limestone at LMH (132.92 m), and it is assigned to the Mississippian uppermost *sandbergi* Zone. One sample (GCD-1) was taken from Lower *expansa* Zone strata at the base of the Parting Formation in Glenwood Canyon, 20 km east/northeast of Glenwood Springs, Colorado. Finally, one sample (Gil-M1) was collected from the base of the Mississippian Gilman Sandstone Member of the Leadville Limestone north of the town of Gilman, CO on the east wall of the Eagle River canyon.

These samples yield very similar age distributions, with main age groups of 2.0–1.7 Ga, 1.5–1.4 Ga, and 1.2–1.0 Ga, and subordinate age groups of 2.8–2.5 Ga and 600–400 Ma (Fig. 14; Data Repository 2). A Kolmorgorov–Smirnov (K–S) test, a nonparametric statistical analysis, was performed on the samples to assess statistically significant similarities in provenance. A p-value greater than 0.05 indicates that at a 95% level of confidence the samples cannot be distinguished as coming from separate populations. Two samples, LHU-LF1 and LMH-132.92, are very similar, with K–S p-values of 0.46 (Data Repository 3), whereas the other two samples are less similar due mainly to differing proportions of the main age groups. LHU-LF1 and LMH-132.92 are also similar in yielding 2.09–2.08 Ga zircon grains.

10. Detrital zircons: Interpretations

The age groups present in these samples are an excellent match for the dominant ages of igneous rocks in North America (Hoffman, 1989), and for detrital zircons from Paleozoic strata of the Cordilleran passive margin succession that were derived largely from North American basement assemblages (Gehrels and Pecha, 2014). A comparison of our ages (Fig. 14) with these reference data sets suggests that the ultimate sources for the detrital zircons in our samples are as follows:

- 2.8–2.5 Ga (age peak of 2.715 Ga): derived from the Canadian Shield or the Wyoming Province.

- 2.09–2.08 Ga (age peak of 2.086 Ga): derived from the northwestern Canadian Shield, perhaps the Peace River arch region (see discussion below).
- 1.9–1.8 Ga (age peak of 1.849 Ga): derived from the Canadian Shield or the Wyoming Province.
- 1.8–1.7 Ga (age peaks of 1.785 and 1.714 Ga): derived from the Yavapai Province of southwestern North America
- 1.5–1.4 and 1.4–1.33 Ga (age peaks at 1.552 and 1.378 Ga): derived from the midcontinent igneous province.
- 1.2–1.0 Ga (peak at 1.118 Ga): derived from the Grenville orogen of eastern/southern Laurentia
- 600–400 Ma (main peak at 500 Ma): derived from circum-Laurentia orogenic systems that contain Neoproterozoic–early Paleozoic igneous rocks, including the Caledonian, Appalachian, and perhaps Innuitian and Ouachita orogens.

These interpretations suggest that our samples consist of a mix of detrital zircons ultimately derived from relatively local basement rocks (1.8–1.3 Ga) and from distant sources. Deciphering the dispersal pathways from these distant sources is of course complicated by the likelihood that the zircon grains have been recycled through older sedimentary successions, with multiple episodes of sedimentary transport. The 1.2–1.0 Ga grains in our samples are excellent candidates for multiple episodes of recycling, given that sediment from the Grenville orogen probably blanketed much of North America during Meoproterozoic time (Rainbird et al., 2012). Such 1.2–1.0 Ga grains are consequently found in many North American assemblages that have no direct connection to the Grenville orogen (e.g., Gehrels and Pecha, 2014).

Based on patterns observed in other detrital zircon data sets from western North America, the far-traveled >1.8 Ga and <1.0 Ga zircons in our samples may have experienced three different dispersal pathways. One pathway involves transport of grains from the northern Canadian Shield during the Late Devonian as a result of emergence of the Franklinian/Innuitian orogen (Beranek et al., 2010; Anfinson et al., 2011). Young (600–400 Ma) grains may have been shed from arc systems (e.g., Alexander and Pearya terranes) along the paleo-Arctic margin. An alternative origin for these young grains would be that they were transport from the Caledonian–Appalachian orogen, as has been suggested for the influx of early Paleozoic grains in Devonian–Mississippian strata of the Grand Canyon (Gehrels et al., 2011).

A third possibility is that the >1.8 Ga grains were derived from rocks of the Roberts Mountains allochthon, which are known to contain detrital zircons of the appropriate age and to have sourced much of the sediment in the Antler foreland basin (Gehrels and Dickinson, 2000; Gehrels et al., 2000; Gehrels and Pecha, 2014). Such grains are thought to have been ultimately derived from the Peace River arch region of the northwestern Canadian Shield, and to have been transported southward either tectonically or in off-shelf dispersal systems. Regardless of the specific sources, the repeated development of unconformities within the Late Devonian, illustrated in this study, reflect deposition within the tectonically active Antler basin. Migration of a forebulge within the basin, along with other geodynamic changes produced by convergent tectonics, led to a mixed signal of disparate source rocks, and the complicated stratigraphic architecture and chemostratigraphic signature documented herein.

11. Conclusions

The late Famennian (Late Devonian) to Early Mississippian was characterized by major changes to the atmosphere, biosphere, and oceans as a result of the onset of glaciation, large eustatic sea level fluctuations, a terrestrial plant radiation, and changes to biogeochemical cycling (Walliser, 1984; Johnson et al., 1985; Streel et al., 2000; Joachimski and Buggisch, 2002; Sandberg et al., 2002; Algeo, 2004;

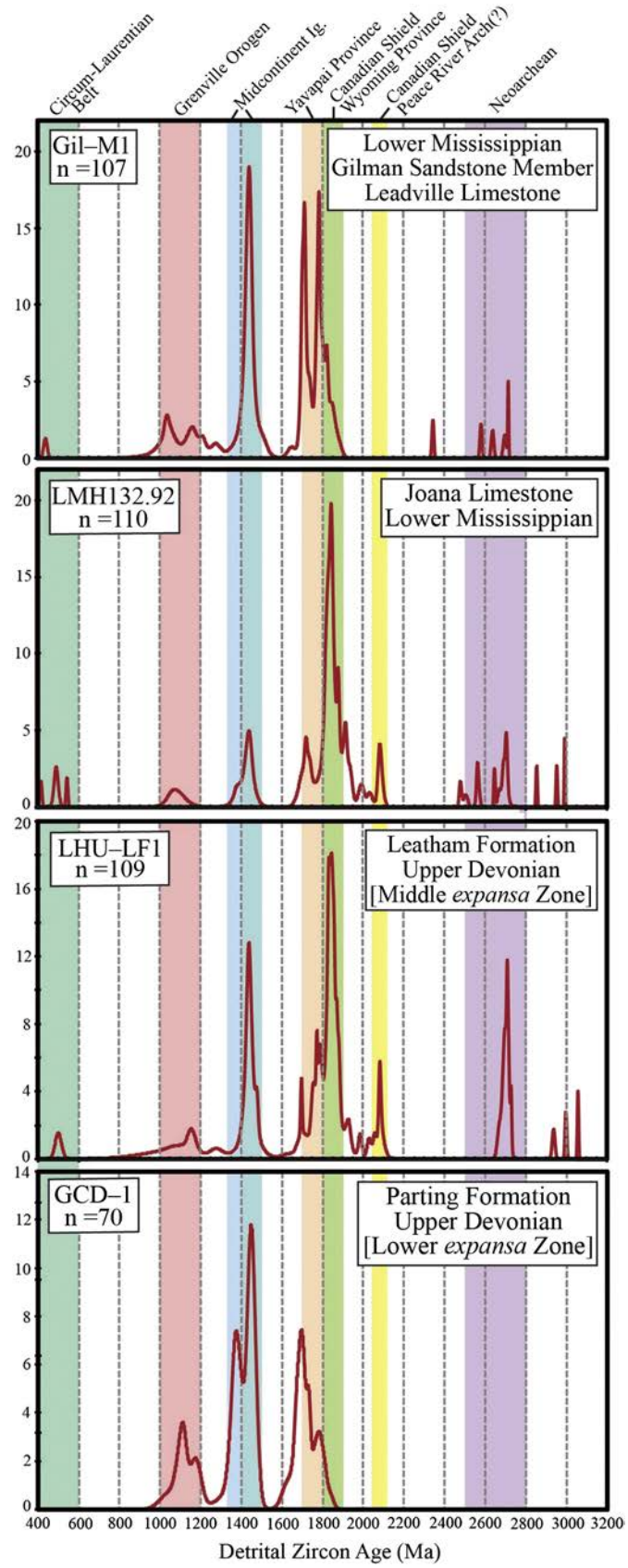

Fig. 14. Detrital zircon relative age probability diagrams for uppermost Devonian and lower Mississippian samples from western Laurentia. The relative age probability diagrams show ages and uncertainty (plotted as a normal distribution about the age).

Brand et al., 2004; Buggisch and Joachimski, 2006; Cramer et al., 2008; Kaiser et al., 2008; Myrow et al., 2011, 2013). Specific global biotic events at this time, generally considered to represent parts of glacial–interglacial cycles (De Vleeschouwer et al., 2013; Myrow et al., 2014), were associated with transgression, oceanic anoxia, and widespread deposition of organic-rich black shale (Berry and Wilde, 1978; House, 1985; Becker, 1993; Walliser, 1996; Caplan and Bustin, 1999; Kump et al., 2005; Racki, 2005; Kaiser et al., 2008).

Upper Devonian to Lower Mississippian strata exposed in Utah and Montana contain a record of global and regional events that occurred during this important interval in Earth history. Upper Famennian strata from Utah (Beirdneau, Leatham, and Pilot Shale formations) and southern Montana (Three Forks and Sappington formations) contain fine-grained siliciclastic and carbonate strata that record regionally significant disconformities, some of which are linked to well-known eustatic and biological events. Transgressive deposits in both Montana and Utah of the *trachytera* Conodont Zone may in part record the Annulata event, which consisted of an extinction event and associated eustatic rise. However, our carbon isotopic data is inconclusive, in large part because the event has a very muted isotopic signal. The later Dasberg event is potentially recorded in our study by an unconformity and shift from Lower *expansa* to Middle *expansa* Zone strata at a very thin sandstone bed below a regionally extensive oncolite unit. Unconformities recorded in more landward sections in Colorado were also developed during this event (Myrow et al., 2013). The strata of this study do not record the transgressive phase of the Dasberg, possibly because of delayed onlap of Middle *expansa* Zone strata onto a basal Dasberg unconformity. The Hangenberg event, also registered in Colorado, is not recorded in the strata of this study area of the Antler foreland basin, largely due to erosion under regional unconformities. Recognition of linked extinction-eustatic events in this tectonically active basin is extremely difficult, in part due to low-amplitude isotopic shifts in some events (e.g., Annulata and Dasberg), and the inability to readily tease out the signal of tectonics from the relative sea level history.

The Devonian–Lower Mississippian boundary interval is missing within both Utah and Montana. The Lower Mississippian *crenulata* Zone strata in these areas record one of the largest positive $\delta^{13}C_{carb}$ isotope excursions of the Phanerozoic, which resulted in part due to drawdown of atmospheric CO_2 and Kinderhookian glaciation.

Detrital zircon spectra from uppermost Devonian to Lower Mississippian strata of Utah and Colorado have peaks between 1650 Ma and 1900 Ma, which record erosion and transport of rocks from the Mazatzal and Yavapai provinces. Grains with ages between 1400 Ma and 1480 Ma were sourced from Middle Proterozoic anorogenic granite bodies of western Laurentia. Minor peaks at ~1100 Ma were sourced from Grenville basement. Finally, peaks between 2050 Ma and 2080 Ma in Utah samples were likely derived from Ordovician rocks of Nevada as multiple-generation grains originally sourced from the Peace River Arch of northwestern Canada. These detrital zircon geochronological data reflect regional uplift, erosion, and deposition within the tectonically active Antler basin during the Devonian–Mississippian boundary interval. Convergent tectonics and eustatic changes within the evolving backbulge led to widespread dispersal of heterogeneous detrital zircon populations, an irregular pattern of development of unconformities, and a complicated stratigraphic architecture and chemostratigraphic signature.

Acknowledgments

We thank Charles Sandberg for his invaluable assistance in helping us locate the sections, and for his help understanding the stratigraphy of these sections. Gehrels acknowledges NSF-EAR-1338353 for support of the Arizona LaserChron Center. The authors thank the two anonymous reviewers and Editor David Bottjer for helping us improve the paper.

Appendix A. Supplementary Data

Supplementary data to this article can be found online at http://dx.doi.org/10.1016/j.palaeo.2015.03.014.

References

Algeo, T.J., 2004. Can marine anoxic events draw down the trace element inventory of seawater? Geology 32, 1057–1060.

Algeo, T.J., Scheckler, S.E., 1998. Terrestrial–marine telecommunications in the Devonian; links between the evolution of land plants, weathering processes, and marine anoxic events. Philosophical Transactions — Royal Society of London Biological Sciences vol. 353 pp. 113–130.

Algeo, T.J., Scheckler, S.E., Maynard, J.B., 1995. Late Devonian oceanic anoxic events and biotic crises: "rooted" in the evolution of vascular land plants? GSA Today 5, 64–66.

Anfinson, O.A., Leier, A.L., Embry, A.F., Dewing, K., 2011. Detrital zircon geochronology and provenance of the Neoproterozoic to Late Devonian Franklinian Basin, Canadian Arctic Islands. Geol. Soc. Am. Bull. 124, 415–430.

Becker, R.T., 1993. Anoxia, eustatic changes, and Upper Devonian to Lowermost Carboniferous global ammonoid diversity. In: House, M.R. (Ed.), The Ammonoidea: Environment. Ecology, and Evolutionary Change: Systematics Association, Special Volume 47, pp. 115–164.

Becker, R.T., House, M.R., 2000. Devonian ammonoid zones and their correlation with established series and stage boundaries. Cour. Forschungsinsitut. Senckenberg. 220, 113–151.

Beranek, L.P., Mortensen, J.K., Lane, L.S., Allen, T.L., Fraser, T.A., Hadlari, T., Zantvoort, W.G., 2010. Detrital zircon geochronology of the western Ellesmerian clastic wedge, northwestern Canada: insights on Arctic tectonics and the evolution of the northern Cordilleran miogeocline. Geol. Soc. Am. Bull. 122, 1899–1911.

Berner, R.A., 1990. Atmospheric carbon dioxide levels over Phanerozoic time. Science 249 (4975), 1382–1386.

Berry, W., Wilde, P., 1978. Progressive ventilation of the oceans — an explanation for the distribution of the Lower Paleozoic black shales. Am. J. Sci. 278, 257–275.

Bless, M.J.M., Becker, R.T., Higgs, K., Paproth, E., Streel, M., 1993. Eustatic cycles around the Devonian–Carboniferous boundary and the sedimentary and fossil record in Sauerland (Federal Republic of Germany). Ann. Soc Géol. Belg. 115, 689–702.

Brand, U., Legrand-Blain, M., Streel, M., 2004. Biochemostratigraphy of the Devonian–Carboniferous boundary global stratotype section and point, Griotte Formation, La Serre, Montagne Noire, France. Palaeogeogr. Palaeoclimatol. Palaeoecol. 205, 337–357.

Brezinski, D.K., Cecil, C.B., Skema, V.W., 2010. Late Devonian glaciogenic and associated facies from the central Appalachian Basin, eastern United States. Geol. Soc. Am. Bull. 122, 265–281.

Bruckschen, P., Veizer, J., 1997. Oxygen and carbon isotopic composition of Dinantian brachiopods: paleoenvironmental implications for the Lower Carboniferous of western Europe. Palaeogeogr. Palaeoclimatol. Palaeoecol. 132, 243–264.

Budai, J.M., Lohmann, K.C., Wilson, J.L., 1987. Dolomitization of the Madison Group, Wyoming and Utah overthrust belt. Am. Assoc. Pet. Geol. Bull. 71 (7), 909–924.

Buggisch, W., Joachimski, M.M., 2006. Carbon isotope stratigraphy of the Devonian of central and southern Europe. Palaeogeogr. Palaeoclimatol. Palaeoecol. 240, 66–88.

Buggisch, W., Joachimski, M.M., Sevastopulo, G., Morrow, J.R., 2008. Mississippian $\delta^{13}C_{carb}$ and conodont apatite $\delta^{18}O$ records — their relation to the Late Palaeozoic glaciation. Palaeogeogr. Palaeoclimatol. Palaeoecol. 268, 273–292.

Caplan, M.L., Bustin, M.R., 1999. Devonian–Carboniferous Hangenberg mass extinction event, widespread organic-rich mudrock and anoxia: causes and consequences. Palaeogeogr. Palaeoclimatol. Palaeoecol. 148, 187–207.

Caputo, M.V., Crowell, J.C., 1985. Migration of glacial centers across Gondwana during Paleozoic Era. Geol. Soc. Am. Bull. 96, 1020–1036.

Caputo, M.V., de Melo, J.H.G., Streel, M., Isbell, J.L., 2008. Late Devonian and Early Carboniferous glacial records of South America. Geological Society of America Bulletin Special Paper 441 pp. 161–173.

Cramer, B.D., Saltzman, M.R., Day, J.E., Witzke, B.J., 2008. Record of the Late Devonian Hangenberg global positive carbon-isotope excursion in an epeiric sea setting: carbonate production, organic-carbon burial and paleoceanography during the Late Famennian. Geological Association of Canada, Special Publication pp. 103–118.

De Vleeschouwer, D., Rakocinski, M., Racki, G., Bond, D.P.G., Sobien, K., Claeys, P., 2013. The astronomical rhythm of Late-Devonian climate change (Kowala section, Holy Cross Mountains, Poland). Earth Planet. Sci. Lett. 365, 25–37.

Dreesen, R., Paproth, E., Thorez, J., 1988. Events documented in Famennian sediments (Ardenne–Rhenish Massif, Late Devonian, NW Europe). In: McMillan, N.J., Embry, A.F., Glass, D.J. (Eds.), International Symposium on the Devonian System, 2nd, Devonian of the World 2: Canadian Society of Petroleum Geologists, Memoir 14 vol. 2, pp. 295–308.

Gehrels, G.E., Dickinson, W.R., 2000. Detrital zircon geochronology of the Antler overlap and foreland basin assemblage, Nevada. In: Soreghan, M.J., Gehrels, G.E. (Eds.), Paleozoic and Triassic Paleogeography and Tectonics of Western Nevada and Northern California. Geological Society of America Special Paper 347, pp. 57–64.

Gehrels, G., Pecha, M., 2014. Detrital zircon U–Pb geochronology and Hf isotope geochemistry of Paleozoic and Triassic passive margin strata of western North America. Geosphere 10 (1), 49–65.

Gehrels, G.E., Dickinson, W.R., Darby, B.J., Harding, J.P., Manuszak, J.D., Riley, B.C.D., Spurlin, M.S., Finney, S.C., Girty, G.H., Harwood, D.S., Miller, M.M., Satterfield, J.I., Smith, M.T., Snyder, W.S., Wallin, E.T., Wyld, S.J., 2000. Tectonic implications of detrital zircon data from Paleozoic and Triassic strata in western Nevada and northern

California. In: Soreghan, M.J., Gehrels, G.E. (Eds.), Paleozoic and Triassic Paleogeography and Tectonics of Western Nevada and Northern California. Geological Society of America Special Paper 347, pp. 133–150. http://dx.doi.org/10.1130/0-8137-2347-7.133.

Gehrels, G.E., Valencia, V., Ruiz, J., 2008. Enhanced precision, accuracy, efficiency, and spatial resolution of U–Pb ages by laser ablation-multicollector-inductively coupled plasma-mass spectrometry. Geochem. Geophys. Geosyst. 9, Q03017. http://dx.doi.org/10.1029/2007GC001805.

Gehrels, G., Blakey, R., Karlstrom, K., Timmons, M., Dickinson, W., Pecha, M., 2011. Detrital zircon U–Pb geochronology of Paleozoic strata in the Grand Canyon. Lithosphere 3, 183–200.

Giles, K.A., Dickinson, W.R., 1995. The interplay of eustasy and lithospheric flexure in forming stratigraphic sequences in foreland settings: an example from the Antler foreland, Nevada and Utah. SEPM Spec. Publ. 52, 187–211.

Gill, B.C., Lyons, T.W., Saltzman, M.R., 2007. Parallel, high-resolution carbon and sulfur isotope records of the evolving Paleozoic marine sulfur reservoir. Palaeogeogr. Palaeoclimatol. Palaeoecol. 256, 156–173.

Goebel, K.A., 1991. Paleogeographic setting of late Devonian to early Mississippian transition from passive to collisional margin, Antler foreland, eastern Nevada and western Utah. In: Cooper, J.D., Stevens, C.H. (Eds.), Paleozoic Paleogeography of the Western United States — Pacific Section SEPM vol. 57, pp. 401–418.

Gradstein, F.M., Ogg, J.G., Schmitz, M.D., Ogg, G. (Eds.), 2012. The Geologic Time Scale. Elsevier, Amsterdam http://dx.doi.org/10.1016/B978-0-444-59425-9.01001-5 (1144 pp.).

Gutschick, R.C., 1964. Transitional Devonian to Mississippian environmental changes in western Montana. Symposium on cyclic sedimentation: Kansas Geological Survey Bulletin 169 pp. 171–181.

Gutschick, R.C., Rodriguez, J., 1979. Biostratigraphy of the Pilot Shale (Devonian–Mississippian) and contemporaneous strata in Utah, Nevada, and Montana. Geol. Stud. 26, 37–62.

Gutschick, R.C., Suttner, L.J., Switek, M.J., 1962. Biostratigraphy of transitional Devonian–Mississippian Sappington formation of southwest Montana. Billings Geological Society 13th annual Field Conference Guidebook.

Hartenfels, S., Becker, R.T., 2009. Timing of the global Dasberg Crisis — implications for Famennian eustasy and chronostratigraphy. In: Over, D.J. (Ed.), Studies in Devonian Stratigraphy: Proceedings of the 2007 International Meeting of the Subcommission on Devonian Stratigraphy and IGCP 499. Palaeontographica Americana vol. 63, pp. 69–95.

Hoffman, P.F., 1989. Precambrian geology and tectonic history of North America. In: Bally, A.W., Palmer, A.R. (Eds.), The Geology of North America: An Overview: Geological Society of America, Geology of North America. v. A, Boulder, Colorado, pp. 447–512.

House, M.R., 1985. Correlation of mid-Palaeozoic ammonoid evolutionary events with global sedimentary perturbations. Nature 313, 17–22.

House, M.R., 2002. Strength, timing, setting and cause of mid-Palaeozoic extinctions. Palaeogeogr. Palaeoclimatol. Palaeoecol. 181, 5–25.

Isaacson, P.E., Hladil, J., Jian-wei, S., Kalvoda, J., Grader, G., 1999. Late Devonian (Famennian) glaciations in South America and marine offlap on other continents. Abh. Geol. Bundesanst. 54, 239–257.

Isaacson, P.E., Diaz-Martinez, E., Grader, G.W., Kalvoda, J., Babek, O., Devuyst, F.X., 2008. Late Devonian–earliest Mississippian glaciation in Gondwanaland and its biogeographic consequences. Palaeogeogr. Palaeoclimatol. Palaeoecol. 268, 126–142.

Joachimski, M.M., Buggisch, W., 2002. Conodont apatite $\delta^{18}O$ signatures indicate climatic cooling as a trigger of the Late Devonian mass extinction. Geology 30, 711–714.

Joachimski, M.M., Breisig, S., Buggisch, W., Talent, J.A., Mawson, R., Gereke, W., Morrow, J.R., Day, J., Weddige, K., 2009. Devonian climate and reef evolution: insights from oxygen isotopes in apatite. Earth Planet. Sci. Lett. 284, 599–609.

Johnson, J.G., Klapper, G., Sandberg, C.A., 1985. Devonian eustatic fluctuations in Euramerica. Geol. Soc. Am. Bull. 96, 567–587.

Kaiser, S.I., 2005. Mass Extinctions, Climatic and Oceanographic Changes at the Devonian/Carboniferous Boundary. (PhD Dissertation), Bochum, Germany (156 pp.).

Kaiser, S.I., Steuber, T., Becker, T.R., Joachimski, M.M., 2006. Geochemical evidence for major environmental change at the Devonian–Carboniferous boundary in the Carnic Alps and the Rhenish Massif. Palaeogeogr. Palaeoclimatol. Palaeoecol. 240, 146–160.

Kaiser, S.I., Steuber, T., Becker, R.T., 2008. Environmental change during the Late Famennian and Early Tournaisian (Late Devonian–Early Carboniferous): implications from stable isotopes and conodont biofacies in southern Europe. Geol. J. 43, 241–260.

Katz, D.A., Buoniconti, M.R., Montanez, I.P., Swart, P.K., Eberli, G.P., Smith, L.B., 2007. Timing and local perturbations to the carbon pool in the lower Mississippian Madison Limestone, Montana and Wyoming. Palaeogeogr. Palaeoclimatol. Palaeoecol. 256, 231–253.

Kaufmann, B., Trapp, E., Mezger, K., 2004. The numerical age of the Upper Frasnian (Upper Devonian) Kellwasser horizons: a new U–Pb zircon date from Steinbruch Schmidt (Kellerwald, Germany). J. Geol. 112, 495–501.

Korn, D., 2004. The mid-Famennian ammonoid succession in the Rhenish Mountains: the "*annulata* Event" reconsidered. Geol. Q. 48, 245–252.

Kump, L.R., Pavlov, A., Arthur, M.A., 2005. Massive release of hydrogen sulfide to the surface ocean and atmosphere during intervals of oceanic anoxia. Geology 33, 397–400.

Kürschner, W., Becker, R.T., Buhl, D., Veizer, J., 1993. Strontium isotopes in conodonts: Devonian–Carboniferous transition, the northern Rhenish Slate Mountains, Germany. Ann. Soc Géol. Belg. 115, 595–621.

Marynowski, L., Filipiak, P., Zatoń, M., 2010. Geochemical and palynological study of the Upper Famennian Dasberg event horizon from the Holy Cross Mountains (central Poland). Geol. Mag. 147, 527–550.

Mii, H.-S., Grossman, E.L., Yancey, T.E., 1999. Carboniferous isotope stratigraphies of North America: implications for Carboniferous paleoceanography and Mississippian glaciation. Geol. Soc. Am. Bull. 111, 960–973.

Myrow, P.M., 1990. A new graph for understanding colors of mudrocks and shales. J. Geol. Educ. 38, 16–20.

Myrow, P.M., Strauss, J.V., Creveling, J.R., Sicard, K.R., Ripperdan, R., Sandberg, C.A., Hartenfels, S., 2011. A carbon isotopic and sedimentological record of the latest Devonian (Famennian) from the western U.S. and Germany. Palaeogeogr. Palaeoclimatol. Palaeoecol. 306, 147–159.

Myrow, P.M., Hanson, A., Phelps, A.S., Creveling, J.R., Strauss, J.V., Fike, D.A., Ripperdan, R.L., 2013. Latest Devonian (Famennian) global events in western Laurentia: variations in the carbon isotopic record linked to diagenetic alteration below regionally extensive unconformities. Palaeogeogr. Palaeoclimatol. Palaeoecol. 386, 194–209.

Myrow, P.M., Ramezani, J., Hanson, A.E., Bowring, S., Racki, G., Rakociński, M., 2014. High-precision U–Pb age and duration of the latest Devonian (Famennian) Hangenberg event, and its implications. Terra Nova 26, 222–229.

Myrow, P.M., Cole, D., Johnston, D.T., Fike, D.A., Hakim, A., 2015w. Passive transgression: remarkable preservation and spatial distribution of uppermost Devonian (Famennian) nearshore marine facies and fauna of western Laurentia. Palaois (in review).

Nilsen, T.H., Stewart, J.H., 1980. The Antler orogeny — mid-Paleozoic tectonism in western North America. Geology 8, 298–302.

Qie, W.K., Zhang, X.H., Du, Y.S., Zhang, Y., 2011. Lower Carboniferous carbon isotope stratigraphy in South China: implications for the Late Paleozoic glaciation. Science China: Earth Sci. 54, 84–92.

Racka, M., Marynowski, L., Filipiak, P., Sobstel, M., Pisarzowska, A., Bond, D.P.J., 2010. Anoxic Annulata events in the Late Famennian of the Holy Cross Mountains (Southern Poland): geochemical and palaeontological record. Palaeogeogr. Palaeoclimatol. Palaeoecol. 297, 549–575.

Racki, G., 2005. Towards understanding Late Devonian global events: few answers, many questions. In: Over, D.J., Morrow, J.R., Wignall, P.B. (Eds.), Understanding Late Devonian and Permian–Triassic Biotic and Climatic Events: Towards an Integrated Approach: Developments in Paleontology and Stratigraphy. Elsevier, Amsterdam, pp. 5–36.

Rainbird, R., Cawood, P., Gehrels, G., 2012. The Great Grenvillian sedimentation episode: record of supercontinent Rodinia's assembly. In: Busby, C., Azor, A. (Eds.), Tectonics of Sedimentary Basins: Recent Advances. Wiley-Blackwell Publishing, pp. 583–601.

Raymond, A., Metz, C., 2004. Towards ice and its consequences: glaciation in the Late Ordovician, Late Devonian, Pennsylvanian–Permian, and Cenozoic compared. J. Geol. 112, 655–670.

Saltzman, M.R., 2002. Carbon isotope $\delta^{13}C$ stratigraphy across the Silurian–Devonian transition in North America: evidence for a perturbation of the global carbon cycle. Palaeogeogr. Palaeoclimatol. Palaeoecol. 187, 83–100.

Saltzman, M.R., 2003a. Organic carbon burial and phosphogenesis in the Antler Foreland Basin: an out-of-phase relationship during the Lower Mississippian. J. Sediment. Res. 73, 844–855.

Saltzman, M.R., 2003b. Late Paleozoic ice age: oceanic gateway or pCO_2? Geology 31, 151–154.

Saltzman, M.R., 2005. Phosphorus, nitrogen, and the redox evolution of the Paleozoic oceans. Geology 33, 573–576.

Saltzman, M.R., Gonzalez, L.A., Lohmann, K.C., 2000. Earliest Carboniferous cooling step triggered by the Antler orogeny? Geology 28, 347–350.

Saltzman, M.R., Groessens, E., Zhuravlev, A.V., 2004. Carbon cycle models based on extreme changes in $\delta^{13}C$: an example from the lower Mississippian. Palaeogeogr. Palaeoclimatol. Palaeoecol. 213, 359–377.

Sandberg, C.A., 1979. Guide to conodont biostratigraphy of Upper Devonian and Mississippian rocks along the Wasatch Front and Cordilleran Hingeline, Utah. Geol. Stud. 26, 107–132.

Sandberg, C.A., Gutschick, R.C., 1969. Stratigraphy and conodont zonation of type Leatham Formation (Devonian and Mississippian), Bear River Range, Utah. Geological Society of America Abstracts with Programs vol. 1 pp. 70–71.

Sandberg, C.A., Gutschick, R.C., 1978. Biostratigraphic guide to upper Devonian and Mississippian rocks along the Wasatch front and Cordilleran hingeline, Utah. U.S. Geol. Surv. Open File Rep. 78–351.

Sandberg, C.A., Gutschick, R.C., 1979. Guide to conodont biostratigraphy of Upper Devonian and Mississippian rocks along the Wasatch Front and Cordilleran Hingeline, Utah. In: Sandberg, C.A., Clark, D.L. (Eds.), Conodont Biostratigraphy of the Great Basin and Rocky Mountains. Brigham Young University Geology Studies vol. 26, pp. 107–134.

Sandberg, C.A., Klapper, G., 1967. Stratigraphy, age, and paleotectonic significance of the Cottonwood Canyon Member of the Madison Limestone in Wyoming and Montana. Contributions to general geology, 1967. U.S. Geological Survey Bulletin 1251-B, pp. B1–B70.

Sandberg, C.A., Poole, F.G., 1977. Conodont biostratigraphy and depositional complexes of Upper Devonian cratonic-platform and continental-shelf rocks in the Western United States. In: Murphy, M.A., Berry, W.B.N., Sandberg, C.A. (Eds.), Western North America: Devonian. UC Riverside Campus Museum Contribution vol. 4, pp. 144–182.

Sandberg, C.A., Poole, F.G., Gutschick, R.C., 1980. Devonian and Mississippian stratigraphy and conodont zonation of Pilot and Chainman shales, Confusion Range, Utah. In: Fouch, T.D., Magathan, E.R. (Eds.), Paleozoic Paleogeography of the West-central United States, Rocky Mountain Paleogeography. Society of Economic Paleontologists and Mineralogists Symposium 1, pp. 71–79.

Sandberg, C.A., Gutschick, R.C., Johnson, J.G., Poole, F.G., Sando, W.J., 1982. Middle Devonian to Late Mississippian geologic history of the overthrust belt region, Western United States. Rocky Mountain Association of Geologists, Geologic Studies of the Cordilleran Thrust Belt vol. II pp. 691–719.

Sandberg, C.A., Poole, F.G., Johnson, J.G., 1988. Upper Devonian of the western United States. In: McMillan, N.J., Embry, A.F., Glass, D.J. (Eds.), Devonian of the World. Canadian Society of Petroleum Geologists, Memoir 14, pp. 183–220.

Sandberg, C.A., Morrow, J.R., Ziegler, W., 2002. Late Devonian sea-level changes, catastrophic events, and mass extinctions. In: Koeberl, C., MacLeod, K.G. (Eds.), Catastrophic Events and Mass Extinctions: Impacts and Beyond; Boulder, Colorado. Geological Society of America Special Paper 356, pp. 473–487.

Sanz-Lopez, J., Garcia-Lopez, S., Montesinos, J.R., Arbizu, M., 1999. Biostratigraphy and sedimentation of the Vidrieros Formation (middle Famennian–lower Tournaisian) in the Gildar–Montó unit (northwest Spain). Boll. Soc. Paleontol. Ital. 37, 393–406.

Scotese, C.R., 2001. Atlas of Earth History. PALEOMAP Project, Arlington, Texas.

Speed, R.C., Sleep, N.H., 1982. Antler orogeny and foreland basin: a model. Geol. Soc. Am. Bull. 93, 815–828.

Stigall, A.L., 2012. Speciation collapse and invasive species dynamics during the Late Devonian "Mass Extinction". GSA Today 22, 4–9.

Streel, M., Caputo, M.V., Loboziak, S., Melo, J.H.G., 2000. Late Frasnian–Famennian climates based on palynomorph analyses and the question of the Late Devonian glaciations. Earth Sci. Rev. 52, 121–173.

Tasch, P., 1977. Ancient Antarctic freshwater ecosystems, adaptations within Antarctic ecosystems. Proceedings of the Third SCAR Symposium on Antarctic Biology, pp. 1077–1089.

Vannier, J., Thiery, A., Racheboeuf, P.R., 2003. Spinicaudatans and Ostracods (crustacea) from the Montceau lagerstatte (Late Carboniferous, France): morphology and palaeoenvironmental significance. Palaeontology 46, 999–1030 (Part 5).

Wallace, Z.A., Elrick, M., 2014. Early Mississippian orbital-scale glacio-eustasy detected from high-resolution oxygen isotopes of marine apatite (conodonts). J. Sediment. Res. 84, 816–824.

Walliser, O.H., 1984. Pleading for a natural D/C boundary. Cour. Forschungsinsitut. Senckenberg. 67, 241–246.

Walliser, O.H., 1996. Global events in the Devonian and Carboniferous. In: Walliser, O.H. (Ed.), Global Events and Event Stratigraphy in the Phanerozoic. Springer, Berlin, pp. 225–250.

Webb, J., 1979. A reappraisal of the paleoecology of conchostracans (Crustacea: Branchiopoda). Neues Jahrb. Geol. Palaontol. Abh. 158, 259–275.

Wicander, R., Clayton, G., Marshall, J.E.A., Troth, I., Racey, A., 2011. Was the latest Devonian glaciation a multiple event? New palynological evidence from Bolivia. Palaeogeogr. Palaeoclimatol. Palaeoecol. 305, 75–83.

Wilde, P., Berry, W., 1984. Destabilization of the oceanic density structure and its significance to marine "extinction" events. Palaeogeogr. Palaeoclimatol. Palaeoecol. 48, 143–162.

Williams, J.S., 1948. Geology of the Paleozoic rocks, Logan quadrangle, Utah. Geol. Soc. Am. Bull. 59, 1121–1164.

Williams, I.S., 1998. U–Th–Pb Geochronology by ion microprobe. In: McKibben, M.A., Shanks III, W.C., Ridley, W.I. (Eds.), Applications of Microanalytical Techniques to Understanding Mineralizing Processes. Reviews in Economic Geology vol. 7, pp. 1–35.

Ziegler, W., Sandberg, C.A., 1984. Important candidate sections for stratotype of conodont based Devonian–Carboniferous boundary. Cour. Forschungsinsitut. Senckenberg. 67, 231–239.